Sachse, V., Strozyk, F., Anka, Z., Rodrigues, J. F., di Primio, R. (2016): The tectono-stratigraphic evolution of the Austral Basin and adjacent areas against the background of Andean tectonics, southern Argentina, South America. - *Basin Research*, *28*, 4, pp. 462—482.

DOI: http://doi.org/10.1111/bre.12118

The tectono-stratigraphic evolution of the Austral Basin and adjacent areas against the background of Andean tectonics, southern Argentina, South America

V.F. Sachse [(1) (4) (*)], F. Strozyk[(2)], Z. Anka [(1) (5)], J.F. Rodriguez [(3)] and R. di Primio [(1) (6)]

[(1)] GFZ German Research Centre for Geosciences, Section 4.3 Organic Geochemistry, Telegrafenberg, 14473 Potsdam, Germany

[(2)] Energy and Minerals Resources, Geological Institute, RWTH Aachen University, Wüllnerstr. 2, 52056 Aachen, Germany

[(3)] Petrobras Argentina S.A., Buenos Aires, Argentina

now at [(4)] Energy and Minerals Resources, Instititute of Geology and Geochemistry of Petroleum and Coal, RWTH Aachen University, Lochnerstr. 4-20, 52056 Aachen, Germany

now at [(5)] TOTAL Exploration- New Ventures, Paris, France

now at [(6)] Lundin Norway AS, P.O. Box 247, N-1326 Lysaker, Norway

[(*)] Corresponding Author : victoria.sachse@emr.rwth-aachen.de

Abstract

The Austral Basin (or Magallanes Basin) in southern Argentina is situated in a highly active tectonic zone. The openings of the South Atlantic and the Drake Passage to the east and south, active subduction in the west, and the related rise of the Andes have massively influenced the evolution of this area. In order to better understand the impacts of these tectonic events on basin formation to its present-day structure we analyzed 2D seismic reflection data covering about 95.000 km² on- and 115.000 km² offshore (Austral "Marina" and Malvinas Basin). A total of 10 seismic horizons, representing 9 syn- and post- rift sequences, were mapped and tied to well data to analyze the evolution of sedimentary supply and depocenter migration through time. 1D well backstripping across the study area confirms three main tectonic stages, containing (1) the break-up phase forming basement graben systems and the evolution of the Late Jurassic - Early Cretaceous ancient backarc Austral/Rocas Verdes Basin (RVB), (2) the inversion of the backarc marginal basin and the development of the foreland Austral Basin, and (3) the recent foreland Austral Basin. Synrift sedimentation did not exceed the creation of accommodation space, leading to a deepening of the basin. During the Early Cretaceous a first impulse of compression due to Andes uplift

caused rise also of parts of the basin. Controlling factors for the subsequent tectonic development are subduction, balanced phases of sedimentation, accumulation and erosion as well as enhanced sediment supply from the rising Andes. Further phases of rock uplift might be triggered by cancelling deflection of the plate and slab window subduction, coupled with volcanic activity. Calculations of sediment accumulation rates reflect the different regional tectonic stages, and also show that the Malvinas Basin acted as a sediment catchment after the filling of the Austral Basin since the Late Miocene. However, although the Austral and Malvinas Basin are neighboring basin systems that are sedimentary coupled in younger times, their earlier sedimentary and tectonic development was decoupled by the Rio Chico basement high. Thereby, the Austral Basin was affected by tectonic impacts of the Andes orogenesis, while the Malvinas Basin was rather affected by the opening of the South Atlantic.

Keywords: foreland basin; on/offshore correlation; Andes; sedimentation rates; Austral/Malvinas Basin; on/offshore Argentinian continental margin; volcanic activity; basin subsidence

1. Introduction

The Austral Basin (also known as Magallanes Basin) is located on-and offshore in southern Argentina and Chile, in the area of southern Patagonia (Figure 1). The neighboring offshore Malvinas Basin is localized to the east of Tierra del Fuego, on the southernmost continental margin of South America. Several previous studies in both basins have dealt with the evolution (Ludwig *et al.*, 1968; Galeazzi, 1998; Ghiglione, 2002, Ghiglione *et al.*, 2009, 2010; Franzese *et al.*, 2003; Fosdick *et al.*, 2011; Romans *et al.*, 2012; Varela *et al.*, 2012), the petroleum system (Pittion & Gouadain, 1992; Rodriguez *et al.*, 2008; Rossello *et al.*, 2008), the chronostratigraphy (Biddle *et al.*, 1986; Galeazzi, 1998; Pérez Panera, 2012), and presence of magmatic and sedimentary intrusions (Hubbard *et al.*, 2007; Bruni *et al.*, 2008). In the case of the Malvinas Basin, Galeazzi (1998), Tassone *et al.* (2008) and Baristeas *et al.* (2013) carried out a detailed seismo-stratigraphic analysis with focus on the structural-tectonic evolution, as well as the distribution of hydrocarbon leakage features (Baristeas *et*

al., 2012). Various researches (i.e. Galeazzi, 1998; Ghiglione, 2002; Rossello *et al.,* 2008) based on outcrop, well data and scattered seismic lines led to a relatively good knowledge about the basin evolution, however, these studies focused on particular areas of the Malvinas and Austral Basin. In this study we integrate the previous works into a basin-wide view of the processes controlling the evolution of the basin. We present a redefined analysis of the tectono-stratigraphic framework and episodes of basin fill with focus on the northern Austral Basin, but also including the Rio Chico High and the neighboring western Malvinas Basin, based on detailed 2D seismic interpretation and development of a tectono-stratigraphic model. The influence of the rising Andes on exhumation events and sediment supply history of the Austral Basin is a main focus of this study. The investigation of the neighboring Austral Basin and the western Malvinas Basin is used to demonstrate how predominant impacts of regional orogenesis (i.e., Andes formation) affect basin evolution by far-field stresses compared to those from continental break-up and rifting (i.e., Atlantic opening), respectively. The development of the two neighboring basins was not diachronous and initially decoupled by the Rio Chico basement high in terms of sedimentary and tectonic processes. This setting serves as an analogue of the spatial and temporal limitations of tectonic forces on basin systems. Furthermore, a more detailed view inside the Austral Basin demonstrates the sequential evolution of an intra-continental basin from an early rift to a later foreland stage.

1.1 Regional geologic framework

The Mesozoic Austral Basin (or Magallanes Basin, Figure 1) in southernmost Argentina (>50° south latitude) covers an area of approx. 195.000 km^2, both on- and offshore (Zambrano & Urien, 1970). Maximum extent reaches approx. 700 km in length and 370 km in width (Biddle *et al.*, 1986). It is bounded by the Andes in the west (Patagonian cordillera) and south (Fuegian cordillera), the Rio Chico High (Dungeness Arch) in the east, extending as Deseado Massif to the northwest and northeast, as well as the Malvinas Basin in the southeast and the fold & thrust belt in the south. The Austral and Malvinas Basins are part of the South American plate which is surrounded by the Nazca plate to the west, the Antarctic plate to the southwest and south, the Scotian plate to the south and the African plate to the east (Figure 1). In general, South America contains four simplified tectonic provinces from west to

east (Diraison *et al.*, 2000): Cordillera (Fuegian and Patagonian) with metamorphic rocks of Paleozoic and Mesozoic ages, including Jurassic to Mid- Tertiary intrusions and the volcanic arc (1); the remnant marginal Rocas Verdes Basin contains Early Cretaceous marine sediments (2) Austral fold & thrust belt with Paleozoic to Early Cretaceous metamorphic rocks and Mesozoic to Cenozoic sediments (3) and the undeformed Austral Basin to the east (4) (Figure 1; Diraison *et al.*, 2000).

1.2 Stratigraphy

The stratigraphic units are based on the sequences outlined by i.e. Biddle *et al.* (1986), Olivero & Martinioni (2001), Olivero & Malumián (2008), Pérez Panera (2012), Richiano *et al.* (2012) the presented chronostratigraphy was basically compiled by Robbiano *et al.* (1996). For this interpretation best visible markers of stratigraphic units were taken: Tobifera Formation; Lower Inoceramus (Rio Mayer Fm.) and Margas Verdes Formation (Nueva Argentina; not sub-divided); Middle (Arroyo Alfa Formation) and Upper Inoceramus (Cabeza de Leon Fm.); Upper Palermo Aike Formation; Paleocene, Eocene, Oligocene (Lower and Upper Magallanes); Miocene (Santa Cruz and Patagonia; not-subdivided); and Plio-Pleistocene.

1.3 Methods and data set

Seismic data and wells

The study area covers approx. 210.000 km², including parts of the onshore Austral Basin (approx. 95.000km²) and the western offshore Malvinas Basin (approx. 115.000km²) with the Rio Chico High in between (Figure 1). A dense seismic reflection data set consisting of 341 profiles in the onshore and 358 profiles in the offshore area (Figure 2) as well as 140 wells, all provided by Petrobras Argentina S.A., were used for seismic interpretation and subsequent reconstruction of the geological evolution of the Austral Basin. The length of used seismic data for the continental Austral Basin is approx. 5000 km and approx. 12.000 km for the marine part.

The seismic data are standard processed, 2D, industrial reflection seismic profiles (post-stack/time migrated). They consist of different surveys shot between 1970 and 2008

(Malvinas Basin seismic data were recorded between 1970 and 1998). The spacing between single 2D lines varies from 2.5 to 35 km, and the maximum depth of profiles is 8 s TWT. The well data comprises stratigraphic well tops, lithological data, and checkshots. The seismic interpretation and the time-to-depth conversion of interpretation results were performed with Petrel Interpretation Software (Schlumberger).

A seismic-to-well log correlation and its integration with stratigraphic data were carried out to perform a chrono-stratigraphic framework for the basic seismic interpretation, a seismo-stratigraphic interpretation, and a tectono-stratigraphic analysis. In addition to basic stratigraphic seismic horizons, major faults, intrusions, and seismic chimneys were mapped. Seismic horizon interpretation was carried out based on time-migrated well stratigraphy and tracing of corresponding, well visible, continuous reflectors. All seismic horizons and faults were manually interpreted. Due to the partially high spacing between single seismic lines, large parts of the final stratigraphic surfaces were interpolated with a standard interpolation algorithm. Checkshots were used to calculate interval velocities for the interpreted seismic units, summarized to a final velocity model and depth conversion of the interpreted horizons. Velocities are compiled in Table 1. Depth and thickness maps for all seismic units were created. Thicknesses and volumes of seismic units were used to assess sediment distribution and the orientation of sediment input as well as to calculate sedimentation rates.

Sediment accumulation/rates

Sediment accumulation rates ($km^3/Ma*10^{-3}$) were calculated for each unit based on compacted isopach maps, as they show volumetric amounts of sediment covering a specific area. Sedimentation rates (m/Ma) were then calculated from average sediment thicknesses accumulated in defined areas (Table 2). This was done for the entire study area as well as independently for the Austral and Malvinas Basins (Table 2). Note that compaction was not taken into account for this approach, because the present day depth and sediment thicknesses for the entire study area highly vary and thus a consistent change of porosity with depth cannot be assumed. As the sedimentation and accumulation rates were calculated for the entire study area a more precise, decompacted calculation was not done for the entire basins, but for the maximum sediment thickness values of each unit. Based on

this values the sedimentation rates were calculated (Table 3). The porosity values were taken as published by Bond & Kominz (1984) for the lithostratigraphy presented in Figure 3.

1D well backstripping- tectonic subsidence

1D backstripping was done along 38 wells using the "McKenzie tool" included in PetroMod® (Schlumberger). The used wells are located in Figure 4. Thereby the present day stratigraphic record is used to estimate the depth of basement during incremental removing of the sediment and water load (i.e. Watts & Ryan, 1976). The resulting depth reveals the tectonic history of subsidence or uplift as tectonic driven forces in the basin (e.g., Watts & Ryan, 1976). For the back-stripping process the required lithologies, ages, and thicknesses of sedimentary units are provided by internal well reports (Petrobras), while well logs and well picks are based on the seismo-stratigraphic interpretation. Due to compaction of the sediments during deposition and subsidence (Airy isostasy) a decompaction process is assigned during backstripping (see data by Bond & Kominz, 1984; Hantschel & Kauerauf, 2009). Paleo-water depths were adopted from Wilson (1991) as the uncertainty of results for tectonic subsidence in some areas is depending on the paleo-water depth. Thus a deep-water zone was assigned for the Jurassic in the westernmost area of the basin, expanding during the Early Cretaceous to the east, and being pronounced in the central basin during the Late Cretaceous to Paleogene (Figure 5). A theoretical subsidence curve was calculated based on McKenzie (1978), taking into account that extensional basins and accompanied thermal contraction leads to subsidence of the lithosphere and thus creates more space for sediment load followed by further subsidence. The amount of subsidence will depend on the initial amount of stretching. This can be estimated and is known as the stretching factor, or β – factor. β is defined as b/a, whereas b is the stretched width and a the initial width. As the Austral Basin shows a mixture of smooth rifting and flexure, a maximum sediment thickness of 7 km and an assumed crustal thickness of 35 km, we assigned a β-factor of 1.3 for all theoretical models.

2. Results

2.1 Seismo-stratigraphic units, basin geometry and sediment distribution

Seismo-stratigraphic syn- and post- rift sequences were identified and mapped on- and offshore the northern Austral Basin and in the Malvinas Basin. In total 10 seismic horizons, representing nine key stratigraphic units of the study area, were mapped (Figures 3, 6, and 7). These units are (i) pre-Jurassic basement (U1), (ii) Jurassic Tobifera Formation (U2), (iii) Early Cretaceous deposits (Lower Inoceramus and Margas Verdes Formation; U3), (iv) Late Cretaceous deposits (Middle and Upper Inoceramus; U4), (v) sub-unit Coniacian to Campanian deposits (Upper Palermo Aike Formation; U4A), (vi) Paleocene deposits (U5), (vii) Eocene deposits (U6), (viii) Oligocene deposits (U7), (ix) Miocene deposits (U8), and (x) Plio-Pleistocene deposits (U9). In general, the Palaeozoic geometries of the Austral Basin and the western Malvinas Basin follow the structure of basement highs. The Malvinas Basin, on the eastern flank of the basement high Rio Chico, has an approximately triangular shape, while the Austral Basin on the western flank of the Rio Chico High shows an elongated to rhombic geometry (Figures 1 and 7A). The overall maximum sediment thickness, including Mesozoic and Cenozoic is 8000 m (Figure 8).

Acoustic Basement (U1)

The acoustic basement represents pre-Jurassic rocks and is defined by its chaotic to transparent seismic reflectivity (U1) (Figure 7A). The top of the rifted unit occurs as a discontinuous reflector of low to medium amplitudes, which was affected by intense faulting, and shows graben and half-graben structures (Figure 6). The graben structures, including rotated blocks, are observed in the entire study area, except for the Rio Chico High.

On the Rio Chico High and the northern parts of the Austral and Malvinas Basins, the top of U1 occurs in < 1000 m depth, while in the northern Malvinas Basin and the Austral Basin, it is located between 800 and 2000 m with a general deepening trend to 7 km towards the SE and 8 km towards the SW (Figure 7A).

Jurassic synrift (Tobifera Formation) (U2)

The synrift unit is represented by the Jurassic Tobifera Formation (U2), which discordantly overlays the faulted basement and also fills the syn-rift grabens and half-graben structures

(Figure 6). The map of top Jurassic indicates geometries similar to U1 with a general southward deepening trend down to 7 and 7.5 km in the SE and SW parts of the basins, respectively, (Figure 7B). On the Rio Chico High its maximum depth is 800-900 m. The unit shows strong and partly continuous reflection pattern throughout the entire study area. The top reflector is the first continuous reflector of the entire units. The sediments of this unit fill basement grabens and cover the basement, and they are of highly variable thickness (Fig. 6A).

Highest thicknesses are 1494 m, in the western Malvinas Basin, where it forms a prominent, N-S-elongated structure, and 1200 m in the central and southern Austral Basin (Figure 8A). Further, the unit thins out above rotated basement blocks and at the Rio Chico High, where it is of only 250 m thick maximum, thus partially merging with the top basement reflector. Accumulation rate was calculated with 3.24 $km^3/Ma*10^{-3}$ and slightly higher for the Malvinas Basin with 4.49 $km^3/Ma*10^{-3}$ (Table 2 and Figure 9). For the maximum, decompacted thickness a sedimentation rate of 168 m/Ma was calculated (Table 3).

Early Cretaceous (Springhill, Lower Palermo Aike Formation (Lower Inoceramus/Rio Mayer), and Middle Palermo Formation (Margas Verdes Formation/Nueva Argentina) (U3)

The Early Cretaceous (U3) represents a seismic unit with a fashion similar to the Jurassic graben and half graben infill (Figure 7C), while its top reflection is almost continuous across the entire study area. This unit therefore represents the oldest post-rift sediments. The reflector set representing the top of U3 was identified on both sides of the Rio Chico High, but is missing on the Rio Chico High, where a clear differentiation between single reflections of U1, U2 and U3 is limited due to a strong thinning of the entire sediment succession (U1 to U9). Below the top reflector, the reflectors become more diffuse, discontinuous and transparent. The minimum depth of top U3 with approx. 800 m occurs in the northern basins and on the Rio Chico High, while its deepest parts of 6 km are located in the southern basins (Figures 7C and 8B). In the western Austral Basin, the sediments occur now in a shallow depth of 1500 m. The sediment thickness of U3 is very similar to U2. The unit thickens in the central part of the Austral Basin to 1000 m and shows a maximum of 3225 m in the south-westernmost edge of the basin (Figure 8B). An U3 thickness of 1000 m is observed for the southernmost and easternmost part of the Malvinas Basin. A general trend of southward thickening and deepening is observed (Figures 7C and 8B), although it appears generally

smoother and more NW-SE oriented than for the underlying units. An accumulation rate of 0.97km³/Ma*10-³ was calculated, for the Austral/ previous RVB and lower values of 0.69 km³/Ma*10^{-3} for the Malvinas Basin (Table 2; Figure 9). For the maximum, decompacted thickness a sedimentation rate of 116 m/Ma was calculated (Table 3).

Late Cretaceous (upper parts of Middle Palermo Aike Formation (Middle Inoceramus/Arroyo Alfa), Upper Palermo Aike and lower parts of Lower Magallanes (Upper Inoceramus/ Cabeza de Leon) (U4)

The top of the Late Cretaceous unit (U4) is characterized by the Late Cretaceous (Maastrichtian) unconformity, showing truncated reflections on the top of this unit (Figure 6A). The uppermost Late Cretaceous internal reflectors show minor continuous reflectors with a less strong amplitude. The lower Late Cretaceous reflectors show a strong amplitude, occur parallel to the top reflector and are not internally disturbed (Figure 6). Within the western Malvinas Basin, the unconformity is not clearly resolved and thus the age is questionable (see also Baristeas et al., 2012). In the western part areas of lower depth occur. A pronounced deepening from north to south ceased for U4 and a smooth depth in the central Austral Basin occurs. To the west limited sediment accumulations occur now 800 m above sea level. Further, the clear separation of the Rio Chico High and the basin areas is less resolved compared to the older units. In the Malvinas Basin the Late Cretaceous shows a deepening from 800 m depth in the northwest to 4500 m depth in the southeast (Figure 7E). The unit shows highest thicknesses of 5039 m in the southern Austral Basin, with a thinning to values lower than 4000 m towards the NW (Figure 8D). On the Rio Chico High the unit shows an average thickness of 500 m. Also this unit shows highest thicknesses in the southern study area with an elongation of the thickest part in NW-SE direction.

Upper Palermo Aike Formation (lower parts of Upper Inoceramus/Cabeza de Leon) (U4A)

The Upper Palermo Aike Formation subunit (U4A), as part of the Late Cretaceous, clearly demonstrates thinning onlapping geometries at the Rio Chico High (Figure 6A). In the central Austral Basin parallel, continuous reflectors with a strong amplitude characterize the top (Figure 7E). To the west and eastern basin, an onlapping of the U4A top reflector on older Cretaceous sediments is observed (Figure 6A). Sediments of the U4A are deposited (sub-) parallel to the recent coastline and the Andes, but now a migration of the depocenter to the

southeast is clearly visible (Figure 7D). Highest sediment thickness of approx. 2576 m occur in the southern Austral Basin imaging the prominent NW-SE trending structure, which is now thinning to the northwest (Figure 8C). In the northern study area, the formation has a thickness of up to 300 m. To the west, it onlaps on older Cretaceous units. Same applies for the eastern part of the basin, where reflectors are terminating in a tapering and, thinning geometry (Figure 6). In the Malvinas Basin, the U4A was not mapped because well picks are missing and the units' thickness might be below seismic resolution due to its strong thinning towards the western flank of the Rio Chico High.

The whole Late Cretaceous (including subunit U4A) accumulation rates were calculated as 3.09 $km^3/Ma*10^{-3}$ for the Austral Basin and 1.05 $km^3/Ma*10^{-3}$ for the Malvinas Basin (Table 2; Figure 9). For the maximum, decompacted thickness a sedimentation rate of 205 m/Ma was calculated (Table 3).

Paleocene (lower parts of Lower Magallanes Formation) (U5)

The Paleocene unit (U5) is seismically clearly resolved in the Austral Basin, but not on the Rio Chico High and in the western Malvinas Basin, because of its significant thinning down to less than 50 m and thus below seismic resolution. The entire Paleocene reflectors show a high amplitude, occur parallel to the top reflector and are clearly visible in the Austral Basin. The top U5 shows elevations that reach 400 m depth in the western and north-western fringes of the Austral Basin (Figure 7F). Similar to the Late Cretaceous deepest parts of U5 with 2500 m depth are located in the central part of the Austral Basin (Figure 7F). Local sediments in the western part of the Austral Basin are now 1000 m above sea level. The unit clearly reflects the Malvinas Basin's triangular geometry with a deepening from 700 m in the NW to 3600 m in the SE. In the NW Austral Basin and SE Malvinas Basin the Paleocene reaches thicknesses of up to 1396 m (Figure 8E). The majority of the Austral Basin, the Rio Chico High, and the western Malvinas Basin show in average 100 m thick U5. Accumulation rates of 1.7 $km^3/Ma*10^{-3}$ for the Austral Basin and 1.0 $km^3/Ma*10^{-3}$ in the Malvinas Basin were calculated (Table 2; Figure 9). For the maximum, decompacted thickness a sedimentation rate of 173 m/Ma was calculated (Table 3).

Eocene (upper Lower Magallanes Formation) (U6)

The Eocene unit (U6) is locally very thin in the basins and thus below seismic resolution. Similar to the Paleocene, its top reflector is parallel to the overlying and subjacent reflectors, and almost continuous within the entire study area. It shows in general a high amplitude. On the Rio Chico High a clear identification of these reflectors is limited due to thinning of the entire sediment package with a maximum thickness of 300 m. The geometry of U6 (Figure 7G) images sediments 600 m above sea level in the northwest and western area, showing a deepening to 1300 m depth in the central part of the Austral Basin. The Paleocene at the Rio Chico High shows a depth of 500 m. In the Malvinas Basin, a NW - SE deepening from 600 m to more than 3500 m depth in the southern most edge occurs (Figure 7G). A slightly increased sediment thickness to approx. 1908 m is observed in SW central part of the Austral Basin. In the Malvinas Basin thickest parts of up to 1000 m are observed in for the south-eastern part. In comparison, in the NW part, U6 is thin, with a maximum of thickness of 400 m (Figure 6F). Accumulation rates were calculated with 0.9 $km^3/Ma*10^{-3}$ in the Austral Basin and 0.6 $km^3/Ma*10^{-3}$ in the Malvinas Basin (Table 2; Figure 9). For the maximum, decompacted thickness a sedimentation rate of 101 m/Ma was calculated (Table 3).

Oligocene (Upper Magallanes Formation) (U7)

The top of the Oligocene unit (U7) is defined by a well-resolved continuous reflector with high amplitude. Internal reflectors show partly blank outs. Because of missing well data for this unit in the western Malvinas Basin and it's thinning towards the Rio Chico High (less than 50 m), it could not be mapped over the entire study area and is limited to the western and central part of the Austral Basin (Figure 8G). The U7 depth map shows a depth of 800 m in the western and north-western part, while the north shows a depth of 400 m, and in the south of 900 m (Figure 7H). The deepest parts now occur in the south easternmost edge of the study area and not in the central part anymore (Figure 7H). The highest sediment thickness of up to 1044 m occurs in the western part and as non-uniform deposits in the south central Austral Basin and thin out to 150 m in the northeast. In the northwest, southwest and south the U7 partly shows strong thinning to a maximum thickness of less than 50 m. During Oligocene accumulation rate increased again to 2.79 $km^3/Ma*10^{-3}$ in the Austral Basin (Table 2; Figure 9). For the Malvinas Basin no data is available, as done in our study, Galeazzi *et al.* (1998) and Baristeas *et al.* (2012) mapped the Oligocene as part of the

Miocene sequence. For the maximum, decompacted thickness a sedimentation rate of 197 m/Ma was calculated (Table 3).

Miocene (Patagonia/Santa Cruz Formation) (U8)

U7 is covered by the Miocene (U8). The top reflector is in most areas not resolved, because of vertical seismic limit, but this is the uppermost section where continuous reflectors are not that common as in the previous sections. Mainly, the reflectors show a less strong amplitude and are partly disturbed. The U8 top depth map reveals 1400 m above sea level in the western Austral Basin, decreasing to 250 m above sea level in the north and to the east and deepening to 750 m depth in the south (Figure 7). The structures above sea level, which are located in the western part of the Austral Basin, show a NE-SW trend. A constant depth of 150 m occurs on the Rio Chico High, continuing in the Malvinas Basin in the northern fringe, while to the south-easternmost edge deepening to 1750 m occurs (Figure 7I). The maximum thickness of 800 m occurs in the south-western and central area of the Austral Basin, thinning to 200 m in the north and east, continuing on the Rio Chico High, with minimum values of 30 m (Figure 8H). In the Malvinas Basin U8 thickness in mass to the south up to 3121 m and decreases to the north, north-western and north-eastern fringe, from 250 m, to minimum values of less than 50 m. Sediment accumulation in the Austral Basin was calculated with 1.16 $km^3/Ma*10^{-3}$ and in the Malvinas Basin with 1.75 $km^3/Ma*10^{-3}$, but here it is likely that Oligocene sediments contribute (Table 2; Figure 9). For the maximum, decompacted thickness a sedimentation rate of 170 m/Ma was calculated (Table 3).

Plio-Pleistocene (uppermost parts of Patagonia/Santa Cruz Formation) (U9)

Plio-Pleistocene (U9) is the uppermost mapped unit in the study area. The interpretation depends highly on well pick correlation due to limited vertical seismic resolution in the Austral Basin. Within the western Malvinas Basin, the reflectors are (sub-) parallel to the ocean floor. Top depth map reveals deepest Pleistocene of 500 m depth in the eastern and south-eastern part of Malvinas Basin (Figure 7J). The south-western part and the northern parts show a constant depth of maximum 200 m, continuing on the Rio Chico High and with an average depth of 100 m in the eastern and central Austral Basin. The western Austral Basin shows 1500 m above sea level, similar to Miocene and Oligocene, based on well data interpolation. However the depth map shows that the structures in the western Austral Basin are not constantly located above sea level but show variations in between. On the

western part of the Austral Basin the Plio-Pleistocene sediments thin out and on lap older sediments. Highest thickness of 700 m is observed in the southern part of the Austral Basin and of 1264 m in the south-eastern part of western Malvinas Basin (Figure 8I). On the Rio Chico High, the Plio-Pleistocene shows maximum thickness of only 150 m and remains constant on the northern part of the Malvinas Basin. Accumulation rates were calculated with 2.63 $km^3/Ma*10^{-3}$ for the Austral and 6.09 $km^3/Ma*10^{-3}$ for the Malvinas Basin (Table 2; Figure 9). For the maximum, decompacted thickness a sedimentation rate of 257 m/Ma was calculated (Table 3).

2.2 Faults & seismic anomalies

Analysis of the 2D reflection seismic revealed different structures within the Austral Basin, especially in the north-western and southern part of the study area. These structures have been interpreted as: (1) faults, (2) pipes of seismic discontinuity, (3) pipes of seismic continuity and (4) inclined dykes.

(1) The majority of faults mapped in the study area are found within syn-rift sediments, thus are rift-related and associated to graben and half-graben structures below the break- up unconformity (Figure 6). Their main trend is NNW-SSE to NW-SE and NE-SW. Rooted within the basement they are mostly terminating within or at the base of the Early Cretaceous sediments. A second group of faults is detected in Cretaceous to early Palaeogene sediments. These faults are mainly rift-reactivated growth faults sealed by Tertiary (Neogene) sediments (Figures 6 and 10). A third group of faults are NW-SE and NE-SW orientated and occur in younger sediments (Magallanes and Santa Cruz Fm.) and can be related to older (growth) fault systems (Figures 6 and 10). They seem to be coupled to the doming processes of chimney propagation, distributed over the entire area of the Austral Basin.

(2) Vertical seismic pipes with discontinuity of host rock reflections and internally low seismic amplitude or wipe outs (Figure 10A) are spatially identified in the northern, central, and southern part of the Austral Basin. Their height varies between 100 m and 3000 m. Their width is between 40 and 300 m. Zones of weak and diffuse reflectivity within these structures are typical. Sometimes two or more of these

pipes are laterally connected in depth (Figure 10A). In greater depth the boundaries between the pipe zones and surrounding host rock is diffuse and in many cases the structures' roots cannot be clearly identified. However, the roots are located within basement or syn- or early post-rift sediments. The structures' 3D extension is not resolved due to limitations of the seismic data. Therefore we use satellite images from the study area showing rounded or slightly elliptic craters at surface exactly above the positions of the seismic pipes, thus interpreted to represent their surface exposures (Figure 10B, BB). The surface structures are prominent in the southern basin area between 46.5° S (latitude of the Chile Triple Junction, CTJ) and 52° S, found within a total an area of approx. 4500 km² (Corbella *et al.*, 1996), each covering 0.12 to 0.35 km². As the structures represent the Pali-Aike Volcanic Field, we interpreted the seismic pipes to represent the subsurface dykes of these volcanic events (Figure 3).

(3) Vertical seismic pipes with continuity of host rock reflections occur mainly in the northern and spatially in the southern study area. They represent vertical structures rooted at basement or top Early Cretaceous. Their internal structure is characterized by reflections continuing from the host rock, while they can be of reduced or increased amplitude (i.e., high-amplitude anomalies) in some places. The reflections are internally bending upward and depict sharp, fault-like offsets along the edges of the structures, thus resembling tectonic pop-up structures. Their vertical size of up to 2.5 s reaches the full height of the sedimentary section. Their width ranges from almost 6 km in depth to 3-4 km at surface, where they correlate to doming elevations identified from satellite images (Figure 10B, BB). Internal faulting is observed mostly in the lower parts of these pipes (Figure 10B). In some cases, the intrusions are limited to Late Cretaceous sediments (Palermo Aike Superior Fm.) and Eocene (Upper Magallanes Fm.) to Miocene, and show a more crater-like structure at surface.

(4) Inclined seismic dykes were detected in the fold & thrust belt area in the western Austral Basin and occur at approx. 600 m to 800 m depth (1.5-2 s TWT). Contrasting the seismically weak sedimentary host rock these dykes consist of prominent, high-amplitude reflections imaging a fully discordant and inclined geometry. We further

observe that syn-rift-rooted faults extend up to the inclined dykes. The 3D extension of the dyke is not resolved because of seismic data limitations.

2.3 1D well backstripping and Tectonic subsidence

Based on assigned deep water zones in the Austral Basin (Figure 10; Wilson, 1991;), which were used as input parameter for the 1D models of tectonic subsidence, five well groups were defined, but only four were considered for 1D backstripping (Figure 4): (i) the Late Jurassic to Mid/Late Cretaceous deep water zone (Group A; Figure 11A); (ii) Late Cretaceous to Paleogene deep water zone in the central Austral Basin, not affecting the southern tip of Tierra del Fuego (Group B; Figure 11B); (iii) the former marine platform during Jurassic to Late Cretaceous/ Paleogene (Group C; Figure 11C), never affected by deep water; (iv) the Malvinas Basin which had deep-water conditions mainly during the Late Cretaceous (Group D, Figure 11D). Times of earliest basin inversion / rock uplift observed from 1D backstripping are interpolated as presented in Figure 4. The subsidence history can be divided into three major phases: (1) syn- and initial post-rift phase (Stage I; Figures 12A-C); (2) basin inversion and development of the fold & thrust belt; initiating a foreland phase with a migrating fold & thrust belt (Stage II; Figures 12C-E); (3) smooth rock uplift, followed by tectonic subsidence, leading to new rock uplift, deceleration, or even cessation of tectonic subsidence as in the western Malvinas Basin (Stage III; Figure 11F).

The reconstruction of the tectonic subsidence history from wells located in the previous Jurassic/ Early Cretaceous deep water locations in the Austral Basin reveals a constant subsidence during the rifting phase, gradually slowing down similar to the “McKenzie Model” (McKenzie, 1978; Stage I; Figure 11A). Stage I represents thermal subsidence during syn- rift. Time of deepest burial varies between 90 Ma and 80 Ma. The immediate following basin inversion, smoothes and decreases since 65 Ma. This marks the beginning of Stage II, representing the transition from tensional to compressional tectonic regime (Ghiglione *et al*., 2010). This caused a rock uplift of 1000- 1500 m between deepest burial and today. Stage III is either dominated by slight subsidence followed by a prominent rock uplift since 7 Ma as indicated in wells 1 and 4, or a rather constant rock uplift since 34 Ma as indicated in wells 2 and 3.

Wells located in the previous Late Cretaceous/ Paleogene deep water zone also indicate three stages of subsidence (Figure 11B): during Stage I, after constant, flat- dipping subsidence during the rift phase, a short phases of rock uplift is followed by burial occurred with deepest burial in the Paleogene (Paleocene or Eocene). Again rock uplift occurred since 42 Ma in Stage II. As for the other wells Stage III shows a minor subsidence phase for the Late Oligocene (25 Ma), but decelerates at around 7 Ma leading to a phase of rock uplift again. Also here the amount of uplift is approx. 1500 m. However, we observe a clear shift in timing of subsidence and uplift phases compared to the wells from the Jurassic deep water zone.

Wells located in the former marine platform area in the northern and northeastern Austral Basin reflect the three tectonic stages as well (Figure 11C): in stage I a constant subsidence accompanies the rift phase, followed by smoothing and stabilizing since ca. 70 Ma. During Stage II a rapid rock uplift occurred in the Late Paleocene (60 Ma), followed by a smoother and, continuous second phase of rock uplift. This phase heralds the peak of uplift at approx. 23 Ma. The following tectonic subsidence of Stage III ends in a new phase of rock uplift around 5 Ma a variability of total rock uplift from 50 m to 250 m.

The tectonic subsidence curves reconstructed for the Malvinas Basin reveals tectonic stages which are, except some variation, very similar to those of the Austral Basin. The northernmost well (well 14, Figure 11D) shows constant burial since and during the rift phase (Stage I). It reaches its equilibrium phase (subsidence = sediment accumulation) at 75 Ma, followed by a rock uplift phase between 65 and 33 Ma (Stage II). Here the amount of rock uplift is approx. 1000 m. Since the Early Oligocene a smooth rock uplift follows, ending up in a second phase of equilibrium (15 Ma; Stage III). Wells located in the central- western Malvinas Basin show tectonic subsidence during the rifting phase as well (Stage I). The time of deceleration of basin subsidence is depending on the location, reaching it later in the southernmost wells (67 Ma for well 13, Figure 11D) than in the northern central wells (90 Ma for, well 14). The following Stage II rock uplift starts at approx. 67 Ma, reaching maximum uplift of 1500 m in the northernmost well, and approx. 800 m in the southernmost well.

Wells located on the Rio Chico High (wells 11 and 12) reveal trends of tectonic subsidence similar to those from the western Austral Basin. Deepest burial was reached in the Late

Cretaceous and, followed by constant rock uplift, which smoothed since the Late Eocene/Oligocene and got nearly constant since the Miocene. One well on the western flank of the Rio Chico High (well 11; Figure 11D) indicates that it was nearly unaffected by tectonic subsidence and only minor rock uplift is observed during Early Eocene (50 Ma). This depicts the character of the Rio Chico High as basement high, with reduced crustal thinning, that remained elevated during Mesozoic and Cenozoic due to its higher freeboard (Galeazzi, 1998).

3. Discussion

3.1 Sediment distribution and depocenter evolution

Triassic to Jurassic

The syn-rift phase in the Rocas Verdes Basin (RVB) produced classic graben and half graben structures (Figures 6, 11A & B), which are orientated parallel to the N-S opening of the South Atlantic and the former opening of the Weddell Sea in NNW direction, and are therefore correlated to these events. In contrast to the RVB, the Malvinas Basin shows a NW-SE orientation (Figure 7A), which is most likely related to rotation of neighbouring plates during separation of South America and Antarctica (Diraison *et al.*, 2000). The syn- and early post-rift phases due to the breakup of Gondwana are expressed in constant tectonic subsidence (Stage I) in the back arc RVB and the Malvinas Basin. Because of constant subsidence, accommodation space was created, which exceeded the accumulation rates of Triassic and Jurassic sediments during this stage (Table 1 and Figure 9). The result was active deepening of the basin. Slightly higher accumulation rates occurred in the Malvinas Basin. These differences in sediment accumulation can be explained by varying onsets of rifting and that sediment accumulation occurred only in the active basin depocenter. The Malvinas rift phase was terminated to 168- 150 Ma (Galeazzi, 1998), while rifting in the Rocas Verdes Basin due to the opening of the Weddell Sea was dated to 152 to 142 Ma (Calderón *et al.*, 2007; König & Jokat, 2006). This is supported by Baristeas et al. (2013), assuming an early break-up process between Patagonia, the Antarctic Peninsula, East Antarctica, and the Falkland Plateau, affecting the Malvinas Basin.

Cretaceous

The Early Cretaceous represents a phase of balanced creation of accommodation space and sediment accumulation until early Late Cretaceous (Stage I). This phase was accompanied with tectonic subsidence and minor fault activity (Figure 6). Thereby the tectonic regime changed from extension to compression in the early Late Cretaceous, heralding Stage II as shown in Figure 11, initiated by increased Atlantic ridge activity, increased subduction along the Pacific margin, and, finally, crustal shortening (Dalziel, 1981; Ramos, 1989; Fosdick *et al.*, 2011; Varela *et al.*, 2012).

First, in our study area, the western Austral Basin was affected around 87 Ma (Figures 4, 11A) as indicated by sediment deposition at shallower depth or even above sea level to growing foothill structures and active thrusting in the Patagonian fold & thrust belt (see also Wilson, 1991; Fig. 12). Faults of the syn-rift phase were reactivated and growth upward in the sediments (Figure 6). Fosdick *et al.* (2011) have postulated an onset of the compressional phase using thermochronological data for ~100 Ma for a location north of our study area (51°30`S). Varela *et al.* (2012) revealed a compressional regime older than 96 Ma for a study area close to Tres Lagos (49.5°S) in the north west of our study area. Younger ages (~92 Ma) were estimated by Fildani *et al.* (2003) for a fold and thrust belt in the region of the Torres del Paine National Park and in the Ultima Esperanza Province. Progradation of the contraction to the east is indicated from wells of the central and eastern parts of the northern Austral Basin as the timing of basin subsidence deceleration is shifted to younger times and to the east (Figure 4). Our seismic interpretation proves the deceleration of basin subsidence and inversion of the RVB latest for Upper Palermo Aike Formation (Figures 7D and 8D), while backstripping models for the westernmost wells might support even earlier ages (Figure 4; Figure 11B). However, the eastern Austral Basin was still not affected and remained stable as indicated by absence of reverse faulting or reactivation of faults.

The relatively low accumulation rates in the Austral Basin and the Malvinas Basin during this stage (Table 1) can be explained by the long time span of low basin subsidence, the restriction of accumulation only to the formation of elongated basins in front of the fold & thrust belt, the northeast progradation of the thrust belt and the basin depo-centers sub-parallel to the rising Andes (Figures 6D, 12C, D).

However, onlap geometries of Upper Cretaceous sediments (Upper Palermo Aike) to the east as well as a deceleration of subsidence in the west, as indicated by decreasing sediment thicknesses (Figures 8C, D), indicate drastic changes of the main direction of sediment input from N and E to W latest in the Maastrichtian (see also data by Biddle *et al.*, 1986), depicted by the Upper Cretaceous unconformity (see also Figure 6A). As a late Eocene age of the unconformity (~42.5 Ma; Galeazzi, 1998) is as likely as a Late Cretaceous age (Fish, 2005) for the Malvinas Basin, this further indicates an eastward deceleration of basin subsidence. This can be explained by the eastward growth of the thrust wedge and the equilibrium between accumulation and erosion coexisting with sediment load (Figures 9, 11; Naylor & Sinclair, 2008). The accumulation rate exceeded the rate of creation of accommodation space, leading to a shallower basin and sediment migration to the east. The immediate rock uplift and the lack of a steady state phase in well locations close to the orogenic belt can be explained by the absence of new created accommodation space (Naylor & Sinclair, 2008) maybe accompanied by a sea level drop induced by rock uplift (Baristeas *et al*., 2013). The phases of basin inversion within the Austral Basin (Figure 11 A-C) are assumed as rebound after slab detachment, including elastic flexure of the down-bending plate after rupture (Guillaume *et al.*, 2009). These authors pointed out, that mantle-lithosphere interaction and its impact on dynamic topography changes are needed to explain the strong rock uplift occurring from the Andes to the Atlantic coast. However, it remains unclear if all phases of rock uplift can be interpreted as rebound, but the eastward progradation of basin inversion and rock uplift supports this (Figures 4, 11). Thus, the earliest foreland basin phase in the Austral Basin starts in the Late Cretaceous with an eastward shift of the onset towards the Paleocene due to migration of basin loads (Figures 4, 11), what is also supported by the work carried out by i.e. Fosdick *et al.* (2011) and Varela *et al.* (2012). In addition, various authors describe progradating facies changes due to compression resulting in a foreland stage. For the middle Austral Basin the compressional phase was characterized by Varela *et al.* (2012) as fluvial- estuarine facies progradation from east to west (middle Cenomanian to lower Coniacian age (96-84 Ma)). Sedimentary facies changes in the north of Lake Viedma were dated by Cánessa et al. (2005) to upper Albian to upper Cenomanian age. In the area of the Torres del Paine National Park and in the Última Esperanza Province, the compressional phase marks sedimentary changes from a shelf marine facies to a deep marine facies (Wilson, 1991; Fildani *et al.,* 2003; Fildani & Hessler, 2005; see Fig. 5), and was dated on

approx. 92 Ma (Fildani *et al.,* 2003). New data from Fosdick *et al.* (2011) revealed ages of approx. 100 Ma.

As the data sets of Varela *et al.* (2012) and Fosdick *et al.* (2011) both indicate onset of compression being simultaneously around 100 Ma, our data set clearly demonstrates rejuvenation of the contractional influence to the east.

Paleocene and Eocene

The beginning of the early Cenozoic is marked by on-going rise of the Andes, changes in the convergence rates of the Nazca relative to the South American plate (Thomson *et al.*, 2001; Figure 1), and a shift in the Farallón plate convergence direction toward the north accompanied by an increase in its convergence rate (Ghiglione & Ramos, 2005). During the early Paleocene the plate rearrangements led to transpressive E-W deformation in the Austral Basin (Robbiano *et al.,* 1996). Associated features in the Austral Basin are a progradation of the basin's depo-centers from west to east (Figure 8F), a relatively high sedimentation rate coupled with enduring thermal subsidence (Figures 8F-H) and phases of regression (Figure 9; Haq *et al.*, 1987). The following low Eocene sedimentation rate (Figure 9) is a consequence of the basin inversion of the Cretaceous basin to a Palaeocene-Eocene unconformity in the foreland basin. Associated are progradating depocenters from west to east (Figure 8). Biddle *et al.* (1986) related the asymmetric thickening of the Paleocene to Eocene strata towards the west to crustal shortening, eastward migration of the fold & thrust belt and the Neogene Andean rock uplift. Up to the Paleocene, the Austral Basin catched the majority of sediments coming from the Andes, but due to a new forming extensional regime in the Malvinas Basin, sediment was now also significantly transported and deposited into the Malvinas Basin (Figure 8; Baristeas *et al*., 2013). This new setting is likely related to the opening of the Drake Passage (Ghiglione *et al.*, 2010; Baristeas *et al.*, 2013), incremental creation of accommodation space, and the progressively northward migration of the Fuegian fold & thrust belt (Tassone *et al.*, 2008). During the Late Eocene the tectonic regime changed to compression (Ghiglione *et al.*, 2010), as supported by our rock uplift phases starting at the end of the Eocene (Figure 11).

Oligocene

The Oligocene marks the beginning of Stage III and shows variable patterns of rock uplift and subsidence in the backstripping models (Figure 11). This is still related to low accommodation space and ongoing changes in the tectonic system, now being wrench deforming in the Malvinas Basin and compressional in the Austral Basin (Ghiglione *et al.*, 2010). The subduction direction of Nazca plate relative to South America plate was now more perpendicular to the continent (Quinteros & Sobolev, 2012), accompanied by increasing topographic/ rock uplift in the Andes, known as Quechua phase (Thomson *et al.*, 2001). Results are volcanic fields as identified in the seismic (Figure 10), rock uplift as shown in Figure 11 and deformation of Patagonian fold & thrust belt (Ghiglione *et al.*, 2010). As a consequence of the compressional setting, depocenters were deposited in NE-SW direction parallel to the prograding fold & thrust belt (Figure 8). Since the Late Oligocene/Miocene, phases of subsidence reflect the cessation of progradation of the fold & thrust belt and the development of a passive depo-center (Figure 8; Carbonell *et al.*, 2008).

Miocene

The transition between Oligocene and Miocene is marked by a phase of E-W transpressive deformation, massively influenced by the Chile ridge-Chile trench collision in the western part of Tierra del Fuego approx. 14 Ma ago (Cande & Leslie, 1986). Due to this collision Andes uplift and the deformation of the Patagonian fold & thrust belt was still going on (Ramos, 1989), thus limiting the accomodation space in the Austral Basin and only minor accumulation took place in the central part and the south (Figure 8). Latest since the Miocene (not calculable for Oligocene), sediment accumulation in the Malvinas Basin exceeded those of the Austral Basin (Figures 8H, 9; Table 2), showing that the accommodation space in the Malvinas Basin remained high (Figure 8) and an additional major sediment source established from the south: the Fuegian Andes and the rising Fuegian fold- thrust-belt (Galeazzi, 1998; Baristeas *et al.,* 2013).

The observed seismic pipes in the Austral Basin are likely a consequence of transtensional tectonics along the South American and Scotian plates and associated strike-slip faults of NW-SE direction, resulting in the Magallanes Strait rift system. This Pali Aike volcanic field displays eruptions along ENE-WSW and NW-SE fault systems (D`Orazio *et al.*, 2000).

Pliocene to present day

The latest stages of rock uplift at around 5 Ma (Figure 11) depict the time-lag influence of changes in the stress field due to on-going, oblique convergence of the collision between the Chile ridge and the Chile trench, finally resulting in the subduction of the Chile trench and the opening of an asthenospheric window cancelling the downward mantle motion of the South American plate (Guillaume *et al.*, 2009). Despite this tectonic causes for rock uplift phases, the influence of glaciation and deglaciation processes (Ramos, 2005) in the Patagonian Cordillera since the Late Miocene might play a role, but were not taken into account in our models.

Northward migration of the subduction and collision zone associated with prograding slab window (D`Orazio *et al.*, 2000; Kay *et al.*, 2004; Aragón *et al.*, 2013) are expressed at the locality Pali Aike (Bruni *et al.*, 2008), in the northern Condor Cliff area (Bruni *et al.*, 2008) and the Camusú Aike Volcanic Field (Figure 2; Bruni *et al.*, 2008) and supports the idea of mainly magmatic induced seismic pipes detected in the seismic lines (Figure 10). Further, magmatic activities are supposed as result of steepening of a formally shallow subduction zone and thermal anomalies (Kay *et al.*, 2004). However, based on literature information, most of our identified seismic pipes seem to be related to magmatic activity, but some of them might have another origin, i.e. fluid injection or fluid flowpaths, but this cannot be solved in this context.

Post Miocene sequences show highest sediment accumulations in the Malvinas Basin as indicated by thick progradational sequences which are associated to ongoing northward movement of the Fuegian Andes as the primary sediment source (Figure 8I; Figure 9; Table 1). The Austral Basin could not accumulate significant sediments anymore, thus it is highly likely that the sediments were further transported into the Malvinas Basin.

4. Conclusions

A seismic interpretation study was used to compare the tectono-stratigraphic evolution of the large Austral Basin, the Rio Chico High, and the western Malvinas Basin. The study's results demonstrate that the development of the two neighbouring basin systems was decoupled by the basement high over a long period of time. Seismic analysis, calculated accumulation rates, and 1D backstripping clearly demonstrate the importance of the Andes orogenesis and its far-field stresses on the Austral Basin, with only minor impacts on the Malvinas Basin. Tectonics impacts from the opening of the South Atlantic were not detected in the Austral Basin, but in the Malvinas Basin. The present study supports results from previous studies, but also demonstrates how the development of sediment thickness distribution and sediment geometries within the basins is related to impacts of the Andes orogenesis. Based on our backstripping approach of basin evolution we conclude and support the idea that three main stages occurred. These stages show an eastward deceleration from the Austral Basin to the Malvinas Basin. In contrast to the temporal offsets of tectonic impacts in the Austral Basin, the tectonic deformation in the Malvinas Basin is decoupled by the Rio Chico High and can be linked to process related to the opening of the South Atlantic.

The three main stages of basin evolution are:

1. Stage I represents the synrift phase of the Rocas Verdes Basin accompanied with NNW-SSE to NW-SE and NE-SW faulting related to the opening of the Weddell Sea, indicating features from the South Atlantic opening in the Malvinas Basin. Large sediment input into the rift graben structures in the Rocas Verdes Basin caused initial basin subsidence.

2. Stage II was initiated by Andes uplift since at least the Turonian in the study area. It is characterized by rock and topographic uplift, eastward progradation of the Patagonian fold & thrust belt, high sedimentation rates, decrease of accommodation space, and reorganization of the basins' depo-centres and structures. Since the end of Stage II (Eocene), plate reconfigurations were accompanied with magmatism in the Austral Basin, as indicated by magmatic pipes detected in the study area.

3. Stage III represents a phase after cessation of the approximately eastward Patagonian fold & thrust belt migration. Significant changes in sediment accommodation occurred due to reorganization in the stress field to a transpressional tectonic system that started in the Oligocene, a bidirectional sediment source, and finally sediment overfills in the Austral Basin. The sediment accumulation in the Malvinas Basin exceeds that of the Austral Basin at least since the Miocene. This indicates the Fuegian fold & thrust belt as a new, dominating sediment source.

5. Acknowledgments

This study is funded by the German Research Foundation (DFG) within the priority program SPP 1375 - SAMPLE. We thank editor S. Castelltort and reviewers U. A. Glasmacher, A. Bilmes and an unknown reviewer for helpful comments and suggestions that highly improved our manuscript. Petrobras Argentina S.A. is thanked for providing the seismic profiles, well data, and allowing publication.

6. References

ARAGÓN, E., PINOTTI, L., D` ERAMO, F., CASTRO, A., RABBIA, O., CONIGLIO, J., DEMARTIS, M., HERNANDO, I., CAVAROZZI, C.E., AGUILERA, Y.E. (2013) The Farallon-Aluk ridge collision with South America: Implications for the geochemical changes of slab window magmas from fore- to back-arc. *Geoscience Frontiers*, http://dx.doi.org/10.1016/j.gsf.2012.12.004.

BARISTEAS, N., ANKA, Z., DI PRIMIO, R., RODRIGUEZ, J.F., MARCHAL, D., DOMINGUEZ, F. (2012) Distribution and hydrocarbon leakage indicators in the Malvinas Basin, offshore Argentine continental margin. *Marine Geology*, 332-334, 56-74.

BARISTEAS, N., ANKA, Z., DI PRIMIO, R., RODRIGUEZ, J.F., MARCHAL, D., DOMINGUEZ, F. (2013) New insights into the Seismo-Stratigraphic and Structural evolution of the Malvinas Basin, offshore the southernmost South American Atlantic margin. *Tectonophysics*, EDOC: 20852 | 10.1016/j.tecto.2013.06.009 |

BIDDLE, K.T., ULIANA, M.A., MITCHUM JR., R.M., FITZGERALD, M.G., WRIGHT, R.C. (1986) The stratigraphy and structural evolution of the central and eastern Magallanes Basin, southern South America. *International Association of Sedimentologists*, Special Publication, 8, 41-61.

BOND, G.C. & KOMINZ, M.A. (1984) Construction of tectonic subsidence curves for the early Paleozoic miogeocline, southern Canadian Rocky Mountains; implications for subsidence mechanisms, age of breakup, and crustal thinning. *Geological Society of America Bulletin*, 95, (2), 155–173.

BRUNI, S., D`ORAZIO, M., HALLER, M.J., INNOCENTI, F., MANETTI, P., PÉCSKAY, Z., TONARINI, S. (2008) Time-evolution of magma sources in a continental back-arc setting: the Cenozoic

basalts from Sierra de San Bernardo (Patagonia, Chubut, Argentina). *Geological Magazine*, 145, 5, 714-732.

CALDERÓN, M., FILDANI, A., HERVÉ, F., FANNING, C. M., WEISLOGEL, A., CORDANI, U. (2007) Late Jurassic bimodal magmatism in the northern sea-floor remnant of the Rocas Verdes basin, southern Patagonian Andes. *Journal of the Geological Society,* 164, 1011-1022.

CANDE, S.C. & LESLIE, R.N. (1986) Late Cenozoic tectonics of the Southern Chile Trench. *Journal of Geophysical Research*, 91, 471-496.

CÁNESSA, N.D., POIRÉ, D.G. & DOYLE, P. 2005. Estratigrafía de las unidades Cretácicas de la margen Norte del Lago Viedma, entre el Cerro Pirámides y la estancia Santa Margarita, provincia de Santa Cruz, República Argentina. *Congreso Geológico Argentino*, No. 16. Actas del CD-ROM Artículo 366, 8 p. La Plata.

CARBONELL, P.J., OLIVERO, E.B. & DIMIERI, L.V. (2008) Structure and evolution of the Fuegian Andes foreland thrust-fold belt, Tierra del Fuego, Argentina: Paleogeographic implications. *Journal of South American Earth Sciences*, 25, 417-439.

CORBELLA, H., CHELOTTI, L. & POMPOSIELLO, C. (1996) Neotectonica del rift Jurasico austral en Pali Aike, Patagonia Extrandina, Santa Cruz, Argentina. *XIII Congreso Geológico Argentino y III Congreso de Exploración de Hidrocarburos, Actas*, II, 383–393.

DALZIEL, I.W.D. (1981) Back-Arc Extension in the Southern Andes: A Review and Critical Reappraisal. *Phil. Trans. R. Soc. Lond.*, A 300, 319-335.

DIRAISON, M., COBBOLD, P.R., GAPAIS, D., ROSSELLO, E.A., LE CORRE, C. (2000) Cenozoic crustal thickening, wrenching and rifting in the foothills of the southernmost Andes. *Tectonophysics*, 316, 91-119.

D`ORAZIO, M., AGOSTINI, S., MAZZARINI, F., INNOCENTI, F., MANETTI, P., HALLER, M.J., LAHSEN, A. (2000) The Pali Aike Volcanic Field, Patagonia: slab-window magmatism near the tip of South America. *Tectonophysics*, 321, 407-427.

FILDANI, A., COPE, T.D., GRAHAM, S.A., WOODEN, J.L. (2003) Initiation of the Magallanes foreland basin: Timing of the southernmost Patagonian Andes orogeny revised by detrital zircon provenance analysis. *Geology*, 31, 1081- 1084.

FILDANI, A., ROMANS, B.W., FOSDICK, J.C., CRANE, W.H., HUBBARD, S.M. (2008) Orogenesis of the Patagonian Andes as reflected by basin evolution in southernmost South America. In: *Ores and orogenesis: Circum-Pacific tectonics, geologic evolution, and ore deposits*. (Ed. by J.E. Spencer and S.R. Titley), *Arizona Geological Society Digest,* 22, 259-268.

FILDANI, A. & HESSLER, A.M. 2005. Stratigraphic record across a retroarc basin inversion: Rocas Verdes-Magallanes Basin, Patagonian Andes, Chile. *Geological Society of America Bulletin,* 117, 1596-1614.

FISH, P. (2005) Frontier South, East Falkland basins reveal important exploration potential. *Oil and Gas Journal*, 103, 34–40.

FOSDICK, J.C., ROMANS, B.W., FILDANI, A., BERNHARDT, A., CALDERÓN, M., GRAHAM, S.A. (2011) Kinematic evolution of the Patagonian retroarc fold-and-thrust belt and Magallanes foreland basin, Chile and Argentina, 51°30'S. Geological Society of America Bulletin, 123(9-10), 1679–1698.

FRANZESE, J., SPALLETTI, L., GÓMEZ PÉREZ, I., MACDONALD, D. (2003) Tectonic and paleoenvironmental evolution of Mesozoic sedimentary basins along the Andean foothills of Argentina (32°–54°S). *Journal of Earth Sciences*, 16, 81-90.

GALEAZZI, J.S. (1998) Structural and Stratigraphic Evolution of the Western Malvinas Basin, Argentina. *AAPG Bulletin*, 82, 4, 596-636.

GHIGLIONE, M.C., 2002. Diques clásticos asociados a deformación transcurrente en depósitos sinorogénicos del Mioceno inferior de la Cuenca Austral. *Revista de la Asociación Geológica Argentina*, 77, 2, 103-118.

GHIGLIONE, M.C. & RAMOS, V.A. (2005) Progression of deformation and sedimentation in the southernmost Andes. *Tectonophysics*, 405, 25-46.

GHIGLIONE, M.C., SUAREZ, F., AMBROSIO, A., DA POIAN, G., CRISTALLINI, E.O., PIZZIO, M.F., REINOSO, R.M. (2009) Structure and evolution of the Austral Basin fold-thrust belt, southern Patagonian Andes. *Revista de la Asociación Geológica Argentina*, 65,1, 215-226.

GHIGLIONE, M.C., QUINTEROS, J., YAGUPSKY, D., BONILLO-MARTÍNEZ, P., HLEBSZEVTICH, J., RAMOS, V.A., VERGANI, G., FIGUEROA, D., QUESADA, S., ZAPATA, T. (2010) Structure and

tectonic history of the foreland basins of southernmost South America. *Journal of South American Earth Sciences*, 29, 262-277.

GUILLAUME, B., MARTINOD, J., HUSSON, L., RODDAZ, M., RIQUELME, R. (2009) Neogene uplift of central eastern Patagonia: Dynamic response to active spreading ridge subduction? *Tectonics*, 28, doi:10.1029/ 2008TC002324.

HANTSCHEL, TH. & KAUERAUF, A.I. (2009) Pore Pressure, Compaction and Tectonics: Event-Stepping. In: *Fundamentals of Basin and Petroleum System Modeling* (Ed. by T. Hantschel and A.I. Kauerauf). Springer Berlin Heidelberg, p.467.

HAQ, B.U., HARDENBOL, J., & VAIL, P.R. (1987) Chronology of fluctuating sea levels since the Triassic. *Science*, 235, 1156-1166.

HUBBARD, S.M., ROMANS, B.W. & GRAHAM, S.A. (2007) An outcrop example of large-scale conglomeratic intrusions sourced from deep-water channel deposits, Cerro Toro Formation, Magallanes basin, southern Chile, In: *Sand injectites: Implications for hydrocarbon exploration and production* (Ed. by A. Hurst and J. Cartwright), *AAPG Memoir*, 87, 199 – 207.

KAY, S.M., GORRING, M., & RAMOS, V.A. (2004) Magmatic sources, setting and causes of Eocene to Recent Patagonian plateau magmatism (36°S to 52°S latitude). *Revista de la Asociación Geológica Argentina*, 59, 4, 556-568.

KÖNIG, M. & JOKAT, W. (2006) The Mesozoic breakup of the Weddell Sea. *Journal of Geophysical Research*, 111, B12102.

LUDWIG, W.J., EWING, J.I. & EWING, M. (1968) Structure of Argentine continental margin. *AAPG Bulletin*, 52, 2337-2368.

MCKENZIE, D. (1978) Some remarks on the development of sedimentary basins. *Earth and Planetary Science Letters*, 40 (1), 25–32.

NAYLOR, M. & SINCLAIR, H.D. (2008) Pro- vs. retro-foreland basins. *Basin Research*, 20, 3, 285-303.

OLIVERO, E.B. & MARTINIONI, D.R. (2001) A review of the geology of the Fuegian Andes. *Journal of South American Earth Sciences*, 14, 175-188.

OLIVERO, E.B. & MALUMIÁN, D.R. (2008) Mesozoic-Cenozoic stratigraphy of the Fuegian Andes, Argentina. *Geologica Acta*, 6, 1, 5-18.

PÉREZ PANERA, J.P. (2012) Nanofósiles calcáreous y bioestratigrafía del Cretácico del sudeste de la cuenca Austral, Patagonia, Argentina. *Ameghiniana*, 49, 2, 137- 163.

PITTION, J.L., & GOUADAIN, J. (1992) Source rocks and oil generation in the Austral basin. 1991. World Petroleum Congress. 13th World Petroleum Congress, October 20 - 25, 1991, Buenos Aires, Brazil.

QUINTEROS, J. & SOBOLEV, S.V. (2012) Why has the Nazca plate slowed since the Neogene? GEOLOGY, G33497.1, doi:10.1130/G33497.1.

RAMOS, V.A. (1989) Andean foothills structures in Northern Magallanes Basin, Argentina. *American Association of Petroleum Geologists*, 73, 887-903.

RAMOS, V.A. & KAY, S.M. (1992) Southern Patagonian plateau basalts and deformation: backarc testimony of ridge collisions. Tectonophysics, 205, 261-282.

RAMOS, V.A. (2005) Seismic ridge subduction and topography: Foreland deformation in the Patagonian Andes. *Tectonophysics*, 399, 73-86.

RICHIANO, S., VARELA, A. , CERECEDA, A., & POIRÉ, D. G. (2012) Evolución Paleoambiental de la Formación Río Mayer, Cretácico Inferior, Cuenca Austral, Provincia de Santa Cruz, Argentina. *Latin American Journal of Sedimentology and Basin Analysis*, 19, 1, 3–26.

ROBBIANO, J.A., ARBE, H. & GANGUI, A. (1996) Cuenca Austral Marina. In: Geología y Recursos Naturales de la Plataforma Continental Argentina (Ed. by V.A. Ramos and M.A. Turic). Congreso Geológico Argentino, No. 13 y Congreso de Exploración de Hidrocarburos, No. 3, Relatorio 17, 323-341. Buenos Aires.

RODRIGUEZ, J.F., MILLER, M. & CAGNOLATTI, M.J. (2008) Sistemas Petroleros de Cuenca Austral, Argentina y Chile. In: *Simposio: "Sistemas Petroleros de las Cuencas Andinas* (Eds: C. E. Cruz, J. F. Rodríguez, J. J. Hechem and H. J. Villar). Instituto Argentino del Petróleo y del Gas. Talleres Trama S.A., Buenos Aires, 1-31.

ROMANS, B.W., FILDANI, A., GRAHAM, S.A., HUBBARD, S.M., COVAULT, J.A. (2010). Importance of predecessor basin history on sedimentary fill of a retroarc foreland basin: provenance analysis of the Cretaceous Magallanes basin, Chile (50-52°S). *Basin Research*, 22(5), 640–658.

ROSSELLO, E.A., HARING, C.E., CARDINALI, G., SUÁREZ, F., LAFFITTE, G.A., NEVISTIC, A.V. (2008) Hydrocarbons and petroleum geology of Tierra del Fuego, Argentina. *Geologica Acta*, 6, 1, 69-83.

TASSONE, A., LODOLO, E., MENICHETTI, M., YAGUPSKY, D., CAFFAU, M., VILAS, J.F., (2008) Seismostratigraphic and structural setting of the Malvinas Basin and its southern margin (Tierra del Fuego Atlantic offshore). *Geologica Acta*, 6, 1, 55-67.

THOMSON, S.N., HERVÉ, F. & STÖCKHERT, B. (2001) Mesozoic-Cenozoic denudation history of the Patagonian Andes (southern Chile) and its correlation to different subduction processes. *Tectonics*, 20, 693–711.

VARELA, A.N., POIRÉ, D.G., MARTIN, T., GERDES, A., GOIN, F.J., GELFO, J.N., HOFFMANN, S. (2012) U-Pb zircon constraints on the age of the Cretaceous Mata Amarilla Formation, Southern Patagonia, Argentina: its relationship with the evolution of the Austral Basin. *Andean Geology*, 39, 3, 359–379.

WATTS, A.B. & RYAN, W.B.F. (1976) Flexure of the lithosphere and continetal margin basins. *Tectonophysics*, 36, 24-44.

WILSON, T.J. (1991) Transition from back-arc to foreland basin development in southernmost Andes: Stratigraphic record from the Ultima Esperanza District, Chile. *Geological Society of America Bulletin*, 103, 98–111.

ZAMBRANO, J.J. & URIEN, C.M. (1970) Geological outlines of the basins in southern Argentina and their offshore extension. *Journal of Geophysical Research*, 75, 1363–1396.

Table 1 Velocity ranges calculated from checkshot data used for time depth conversion.

Depositional Unit	V min/max (m/s)
U9-U7	1365/2759
U6/U5	1760/2971
U4	1999/3268
U3	2211/3388
U2	2192/4300

Table 2 Calculated accumulation and sedimentation rates for each unit based on isopach maps.

Depositional Unit based on Seismic Interpretation	Age (Ma)	Volume (km^3) Austral/ Malvinas /Austral&Malvinas	Duration (Ma)	Accumulation Rate ($km^3/Ma*10^{-3}$) Austral/Malvinas/ Austral&Malvinas	Area (km^2) Austral/Malvinas/ Austral&Malvinas	Sedimentation Rate (m/Ma) Austral/Malvinas /Austral&Malvinas
U9 Plio-Pleistocene	5.3	13.167/30.456/ 43.630	5.3	2.63/6.09/8.72	56.532/106.250/162.767	46.58/57.35/53.57
U8 Miocene	23	24.880/37.567/62.449	21.4	1.16/1.75*/2.91	96.182/106.250/201.924	12.09/16.6*/14.41
U7 Oligocene	33.9	30.499/0/30.500	10.9	2.79/0**/2.79	89.508/0/89.512	31.26/0**/31.17
U6 Eocene	55.8	19.777/13.088/32.935	21.9	0.9/0.6/1.5	96.037/100.3541/96.368	9.4/5.96/7.64
U5 Paleocene	66.5	18.353/10.591/28.945	10.7	1.7/1.0/2.7	95.421/92.401/187.809	17.98/10.71/14.37
U4 Upper Cretaceous	99.6	101.857/34.690/136.567	33.1	3.09/1.05/4.14	105.533/106.250/211.780	29.16/9.86/19.55
U3 Lower Cretaceous	145.5	445.79/31.616/76.216	45.9	0.97/0.69/1.66	105.531/105.115/210.643	9.2/6.55/7.88
U2 Jurassic	156.5	35.606/49.346/84.971	11	3.24/4.49/7.73	105.533/106.250/211.780	30.67/42.22/36.45

*Including Oligocene sediments in Malvinas Basin **No data exists for Malvinas Basin

Table 3 Calculated decompacted thickness values for each unit and corresponding sedimentation rates. The decompacted thicknesses were calculated based on the porosity/depth relation of Bond & Kominz (1984).

Depositional Unit based on Seismic Interpretation	Age (Ma)	Duration (Ma)	Present Day Maximum Thickness	Decompacted Initial Maximum Thickness	Sedimentation Rate (m/Ma) for Maximum Thickness
U9 Plio-Pleistocene	5.3	5.3	1264	1285	257
U8 Miocene	23	21.4	3121	3641	170
U7 Oligocene	33.9	10.9	1044	2157	197
U6 Eocene	55.8	21.9	1908	2226	101
U5 Paleocene	66.5	10.7	1396	1861	173
U4 Upper Cretaceous	99.6	33.1	5039	6802	205
U3 Lower Cretaceous	145.5	45.9	3225	5353	116
U2 Jurassic	156.5	11	1494	1848	168

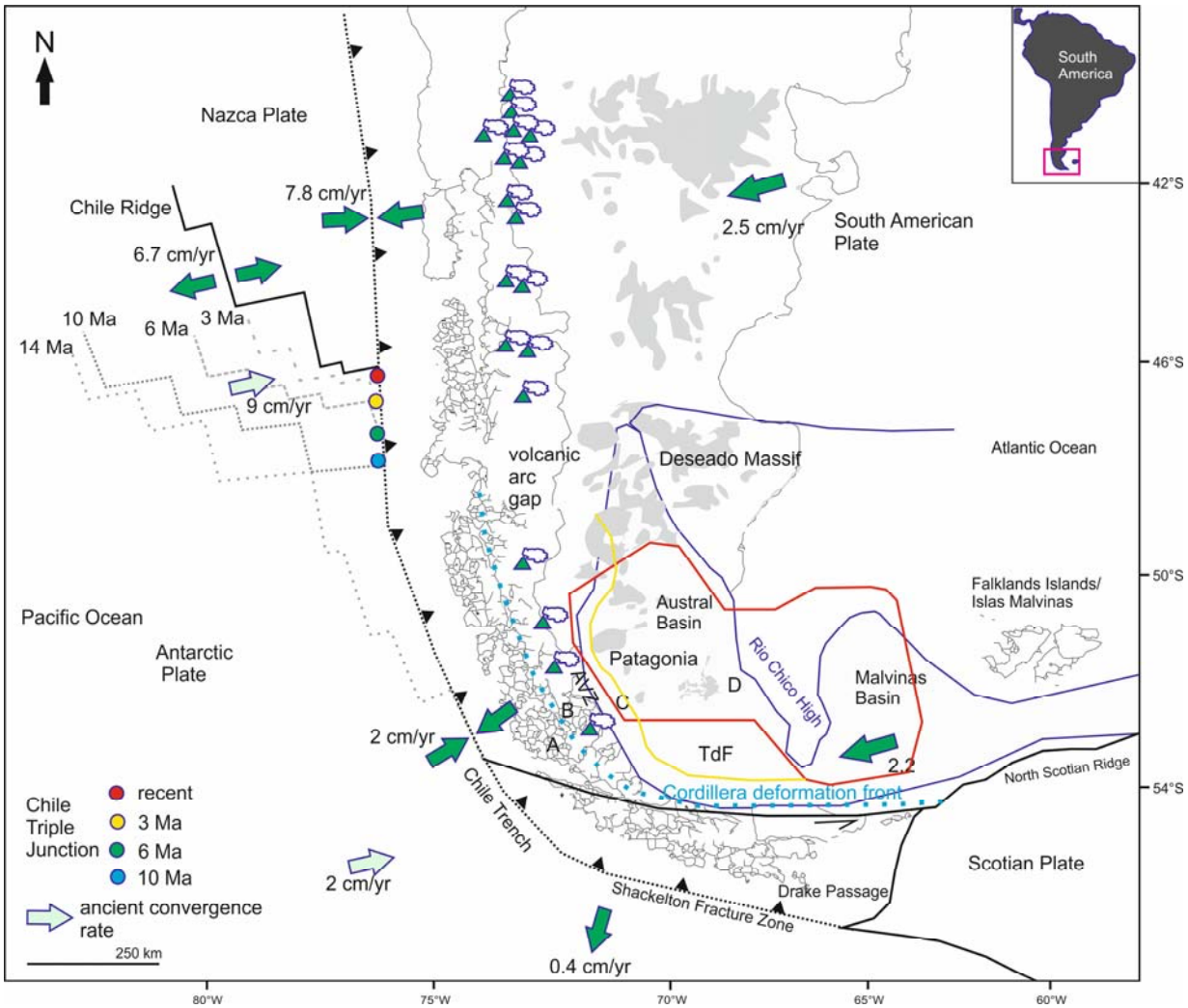

Figure 1 Location of the study area (red polygon), surrounding areas and main geodynamic features. Tectonic provinces A: Andes Cordillera; B: remnant marginal Rocas Verdes Basin; C: fold & thrust belt foot (yellow line); D: undeformed Austral Basin (after Diraison *et al.*, 2000). (TdF: Tierra del Fuego; AVZ: Austral Volcanic Zone). The blue dashed line shows the approx. location of the Cordillera deformation front. The greyish zones represent the Cenozoic Patagonian Plateau lavas (after D`Orazio *et al.*, 2000 and Kay *et al.*, 2004). Positions of Chile triple junction are based on Thompson *et al.* (2001) and Ramos & Kay (1992). Locations of wells for 1D backstripping are included in Figure 4.

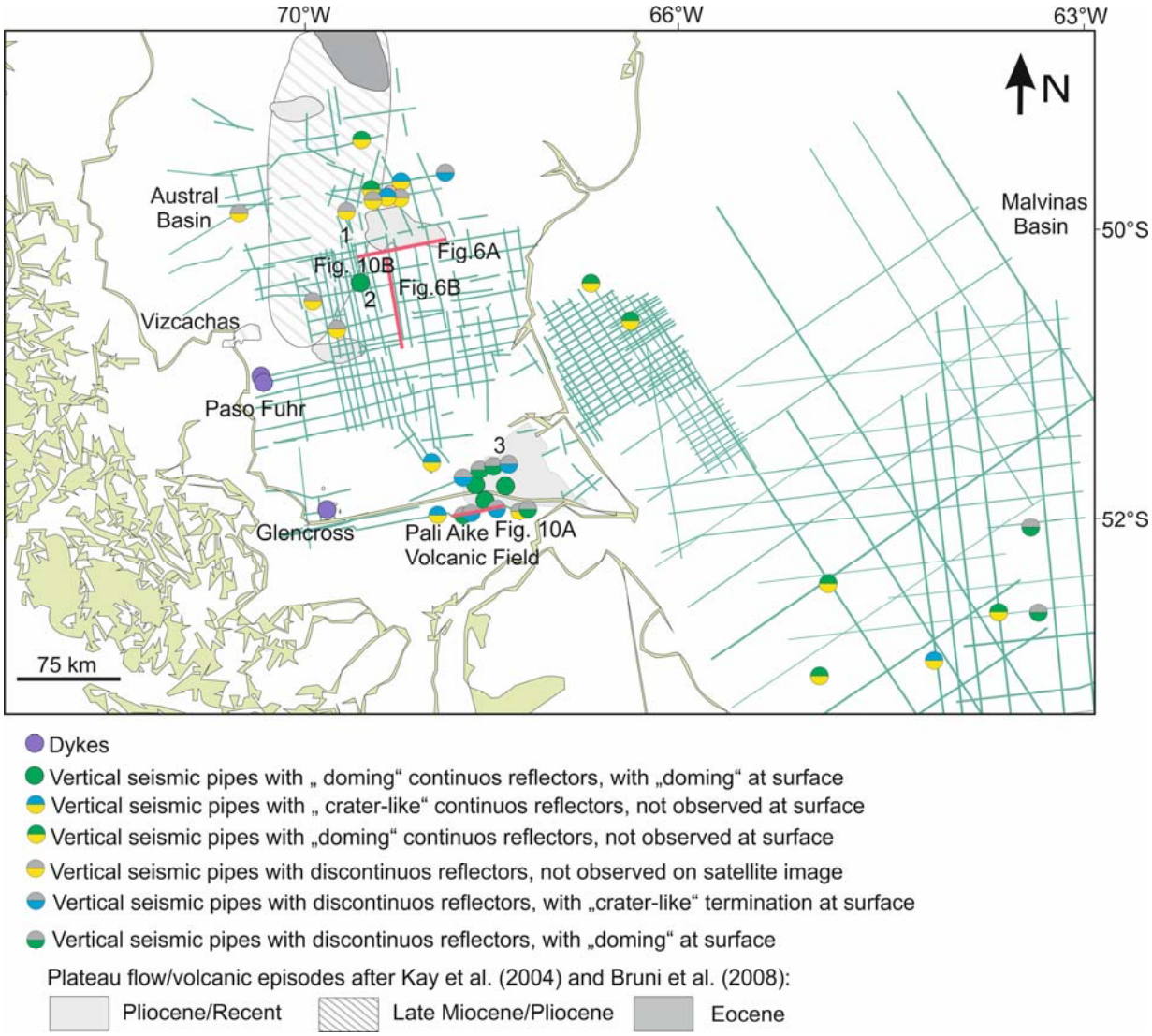

Fig. 2 Location of 2D seismic grid interpreted in this work, observed seismic/satellite images features (Figs. 6, 10) and plateau flows of different ages (after Kay *et al.*, 2004; Bruni *et al.*, 2008). 1: Condor Cliff; 2: Camusú Aike Volcanic Field; 3: Pali-Aike Volcanic Field. Glencross zone hosts Miocene plateau basalts (Bruni *et al.*, 2008). The red lines show the locations of the presented seismic lines.

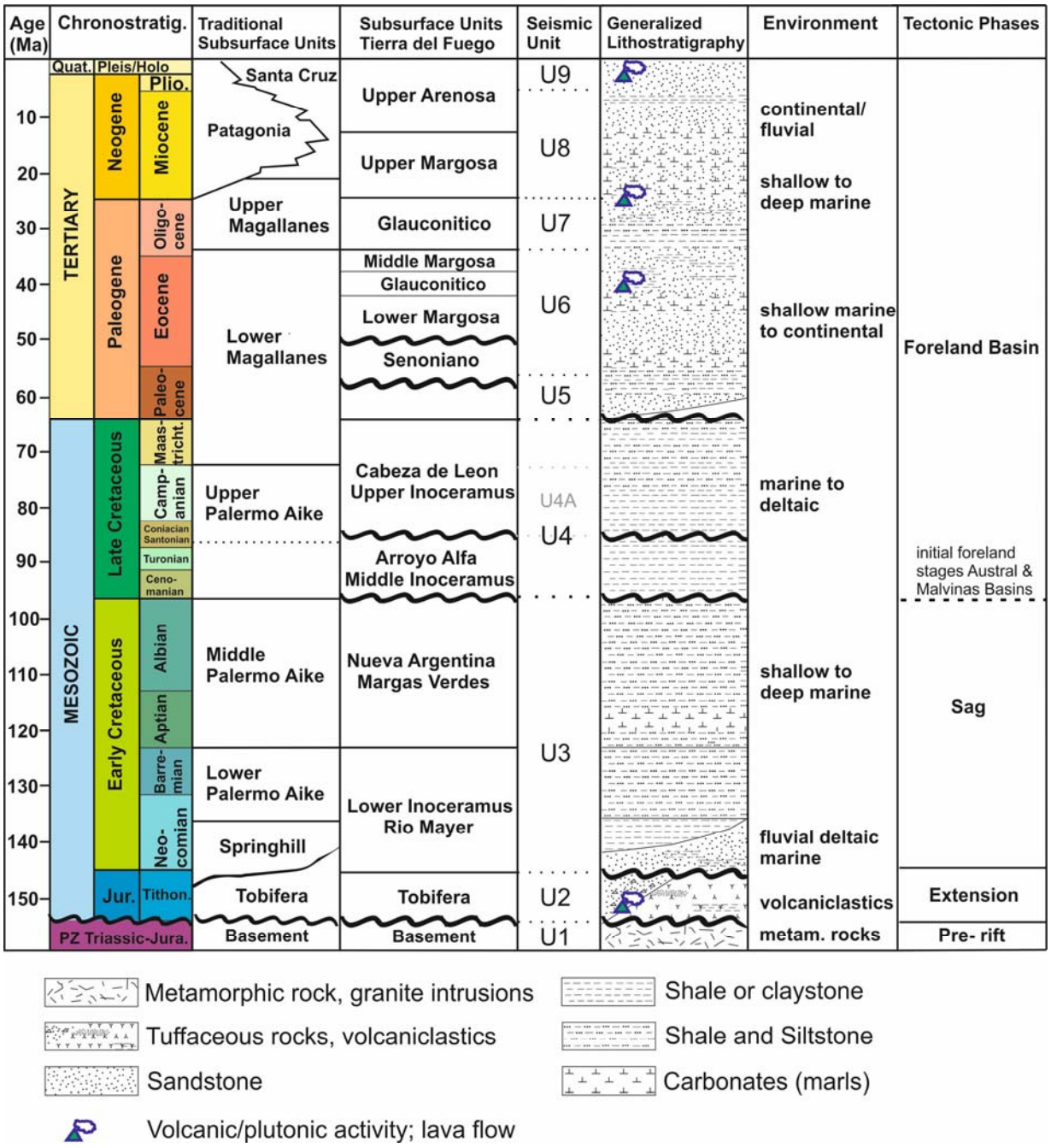

Figure 3Compilation of stratigraphic units, environment, tectonic events, seismo-stratigraphic units identified in this work and key evolution phases of the Austral and Malvinas Basins (compiled from Biddle *et al.*, 1986; Pittion & Gouadain, 1992; Galeazzi, 1998; Franzese *et al.*, 2003 Rodriguez *et al.*, 2008). Interpreted seismic horizons are represented by dotted line.

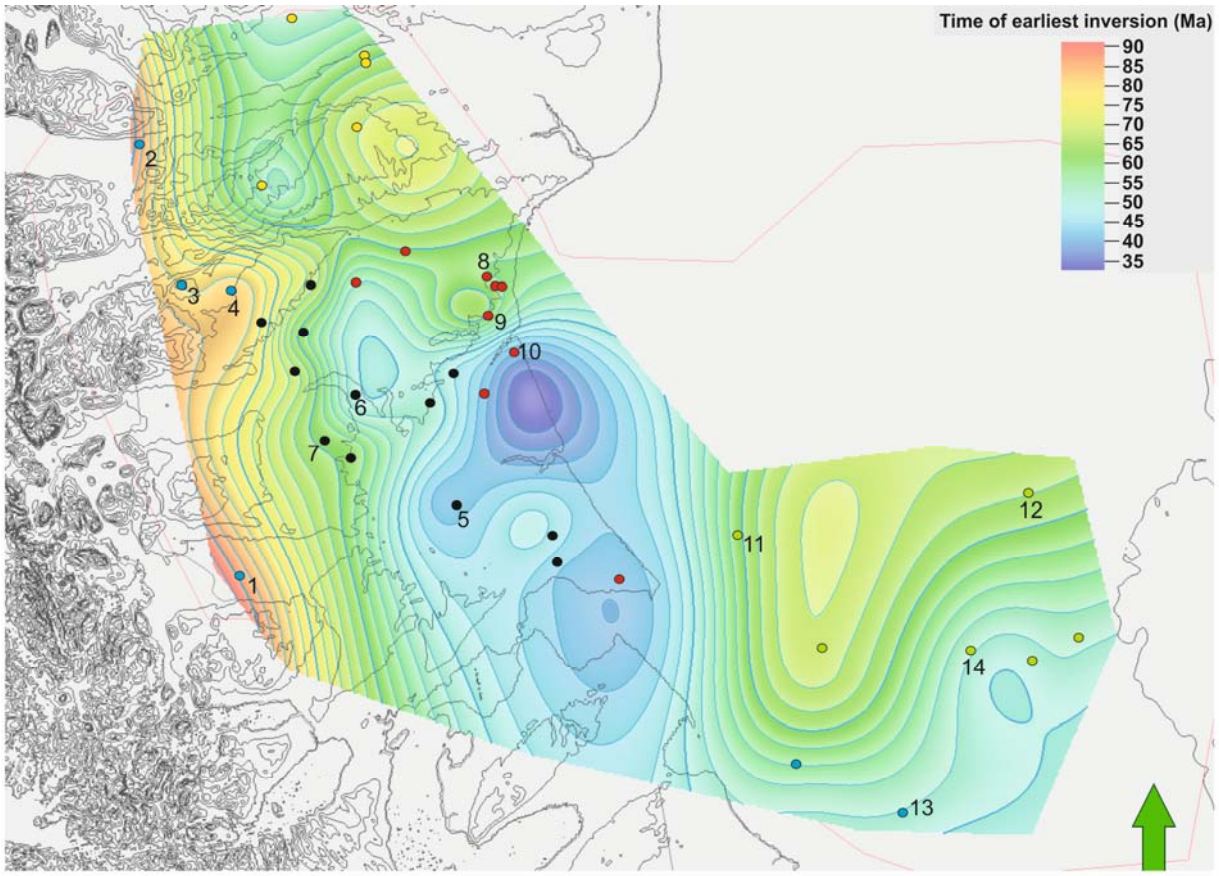

Figure 4 Interpolated distribution of the time of earliest basin inversion based on 38 well 1D backstripping histories. The dots represent the wells used for 1D backstripping as well as their location during deep-water phases. For tectonic subsidence curves see Figure 12 A-D, the numbers represent the tectonic subsidence curves for the respective wells. Assumed deep-water phases were adopted from Wilson (1991).

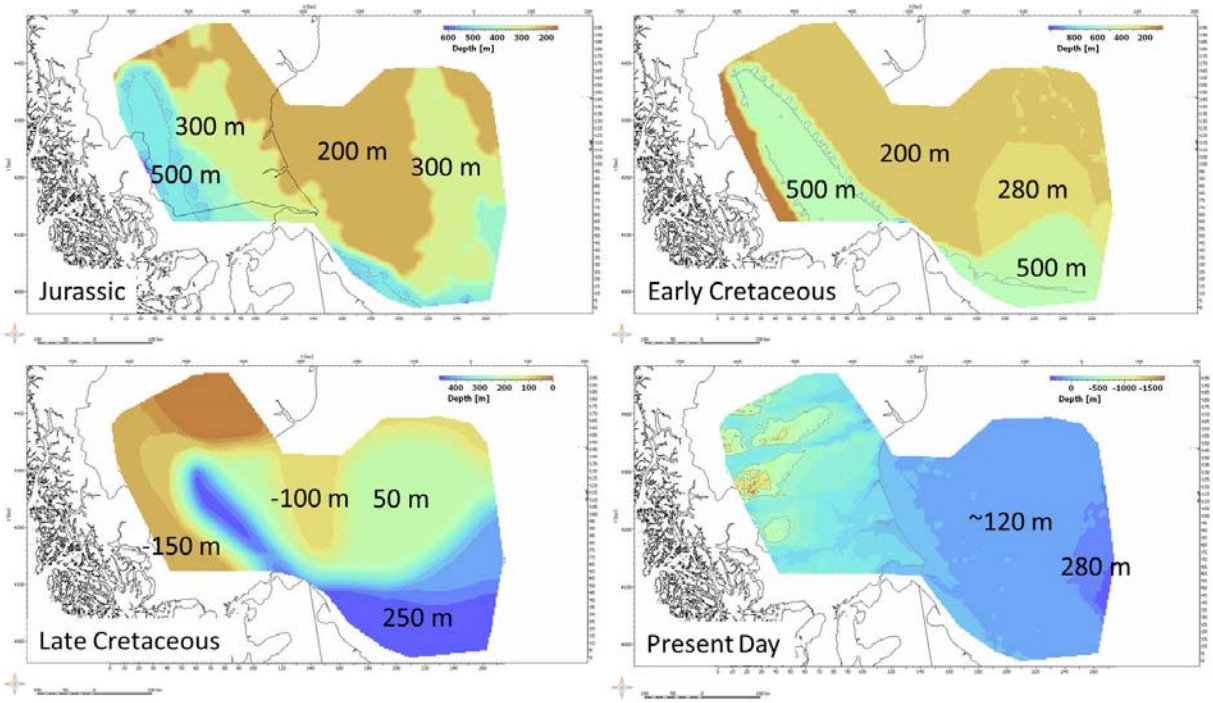

Figure 5. Water depth maps assigned to Jurassic, Early and Late Cretaceous and present day in the Austral and western Malvinas Basin, after Wilson (1991).

A

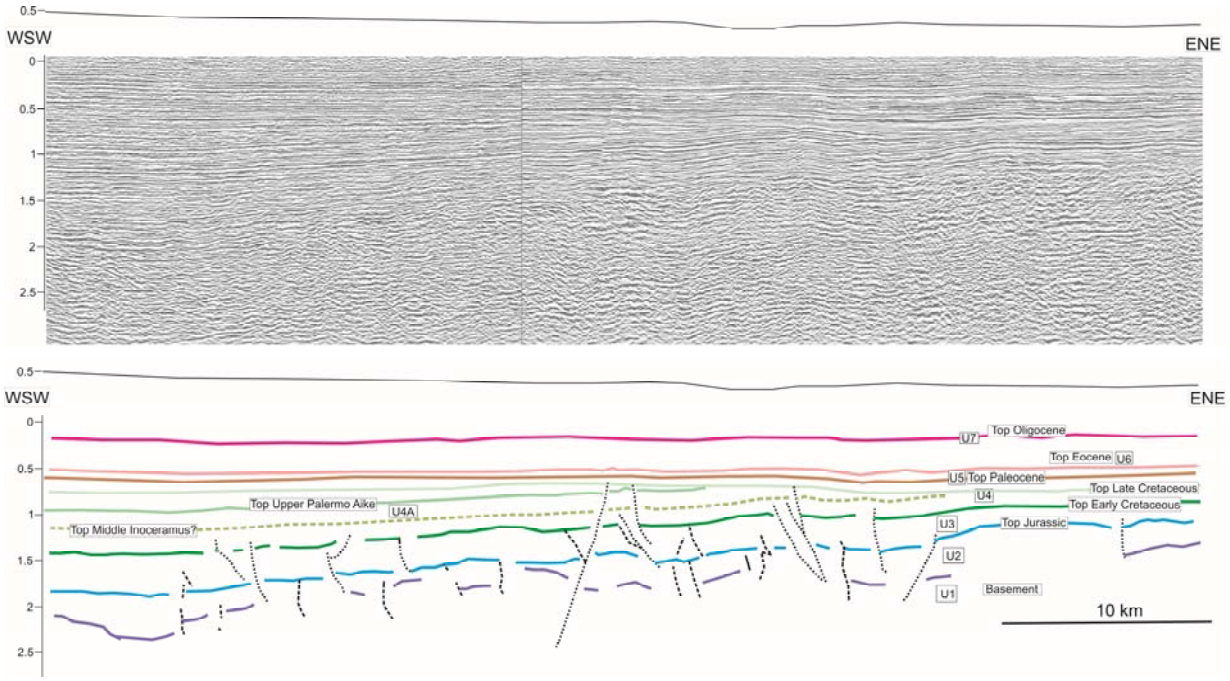

B

Figure 6 A : Interpreted and uninterpreted seismic cross section showing terminating Upper Palermo Aike Formation and suggested terminating Middle Inoceramus depicting the general present-day geometry of the basin.

B: NNW-SSE cross section of the Austral Basin. For locations see Figure 2.

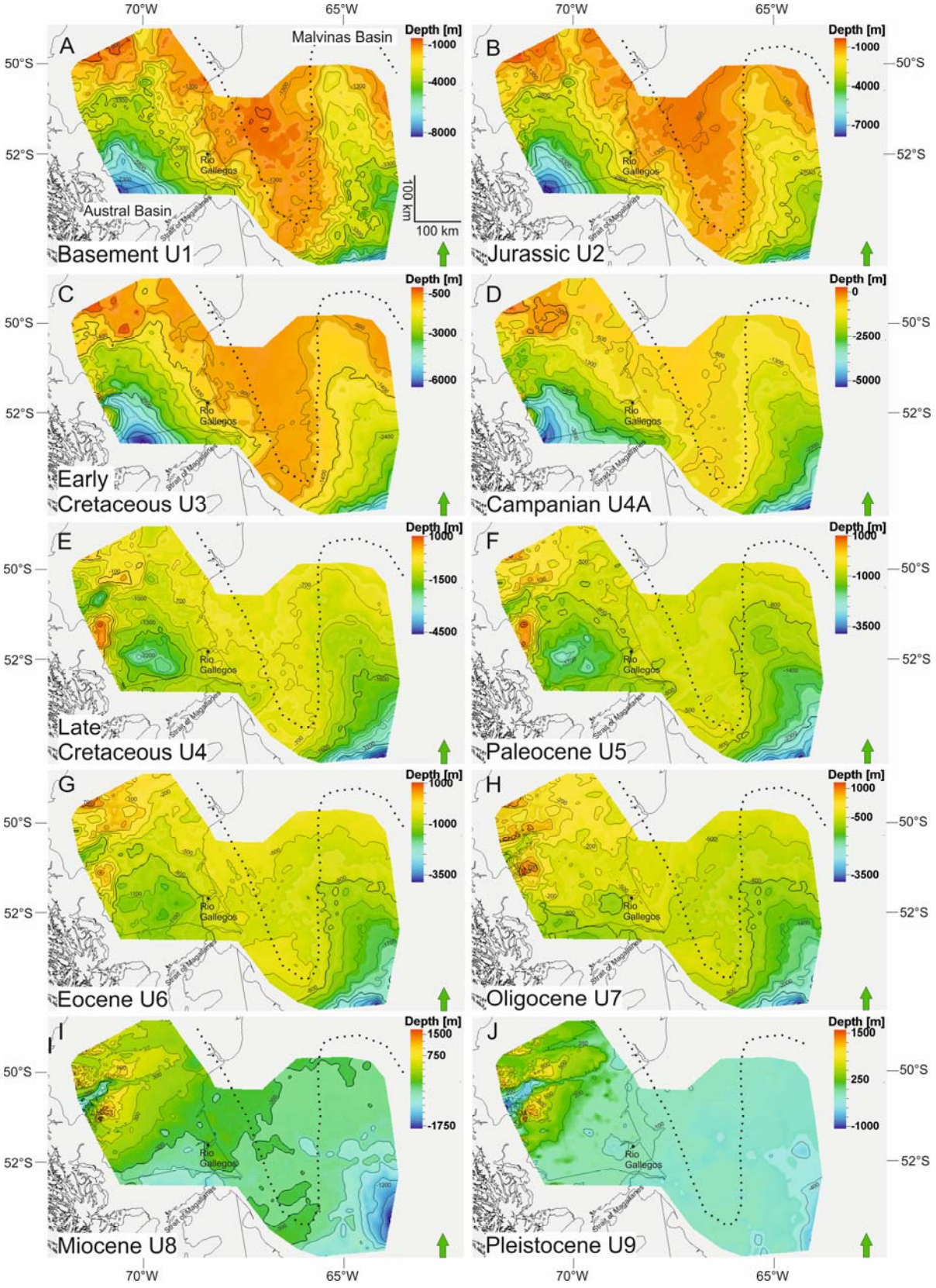

Figure 7 Depth maps of Mesozoic (A-E) and Cenozoic (F-J) top sequences of the Austral and western Malvinas Basins.

Figure 8 Thickness maps (m) of Mesozoic (A-D) and Cenozoic (E-I) sequences of the Austral and western Malvinas Basins. J shows the total thickness of the accumulated sediments in the study area.

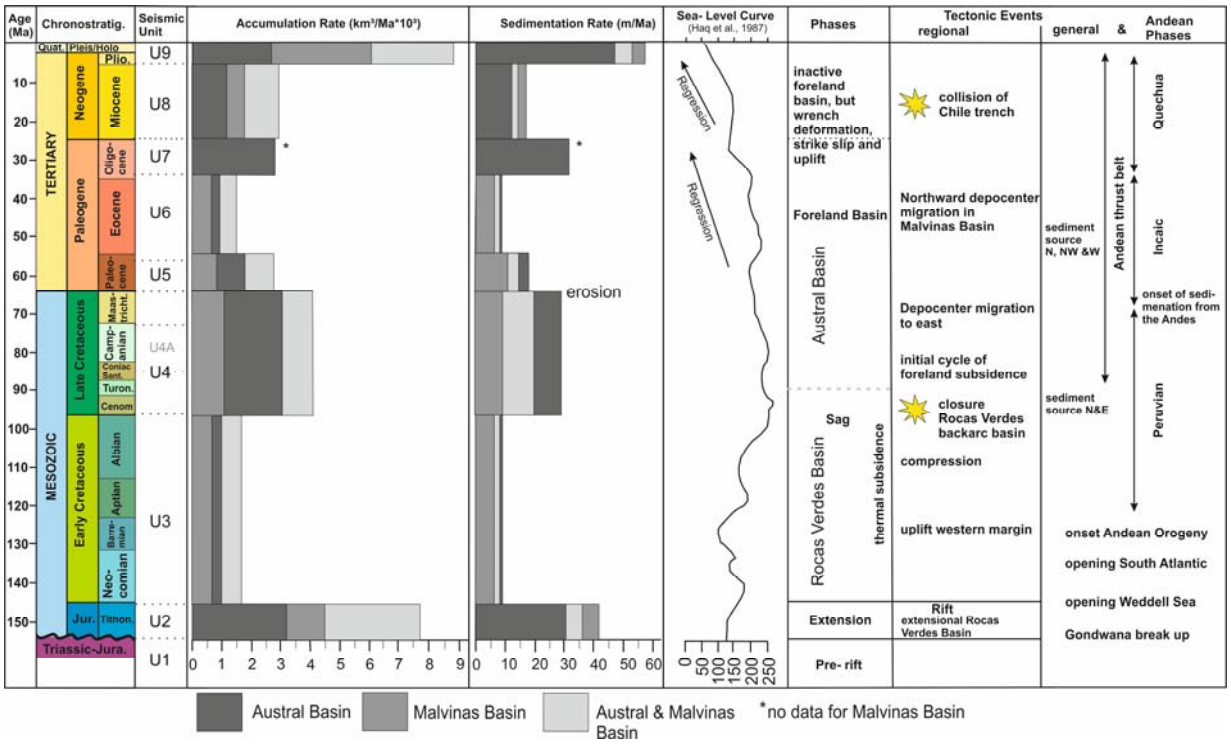

Figure 2 Accumulation and sedimentation rates for the northern Austral Basin, the Rio Chico High and the western Malvinas Basin, as well as the tectonic development of the northern Austral Basin and the sea level curve. As the Rocas Verdes Basin is the precursor basin of the Austral Basin, the Early Cetaceous sediments belong also to the Austral Basin.

Figure 10. Interpreted seismic sections (A) indicating vertical seismic pipes with discontinuous reflectors in the southern part in the Camusú Aike Volcanic Field. (B) vertical pipe with continuous reflectors accompanied by internal faults in the northern basin. Dashed lines represent the structures, black lines associated faults. For location see Figure 2.

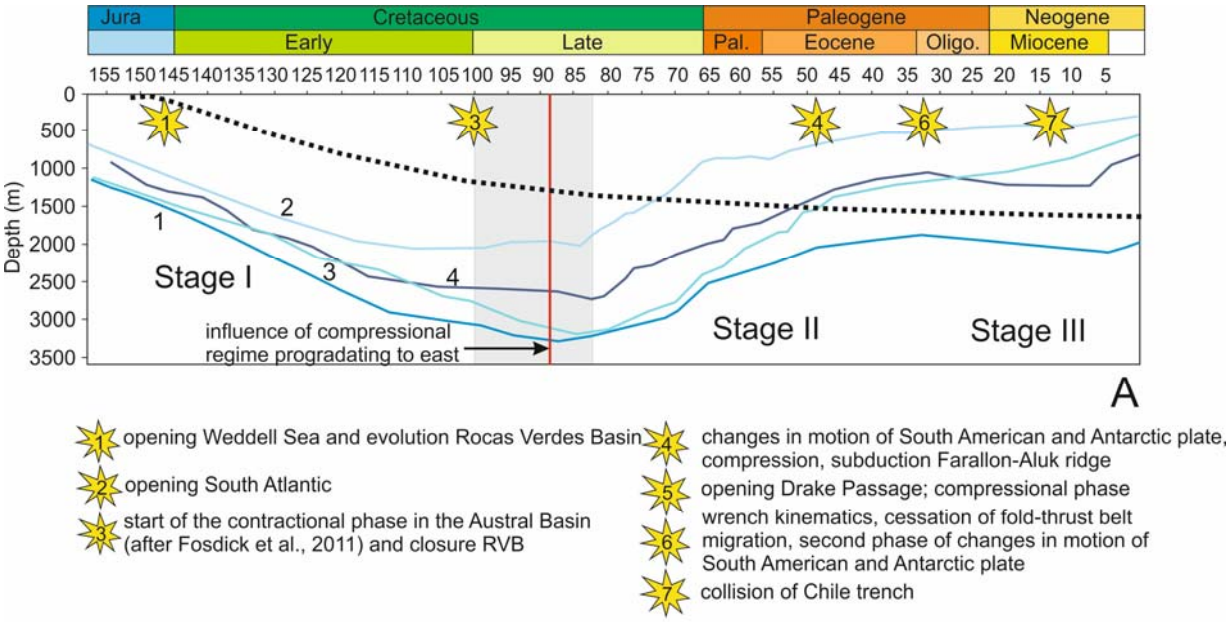

1 opening Weddell Sea and evolution Rocas Verdes Basin

2 opening South Atlantic

3 start of the contractional phase in the Austral Basin (after Fosdick et al., 2011) and closure RVB

4 changes in motion of South American and Antarctic plate, compression, subduction Farallon-Aluk ridge

5 opening Drake Passage; compressional phase

6 wrench kinematics, cessation of fold-thrust belt migration, second phase of changes in motion of South American and Antarctic plate

7 collision of Chile trench

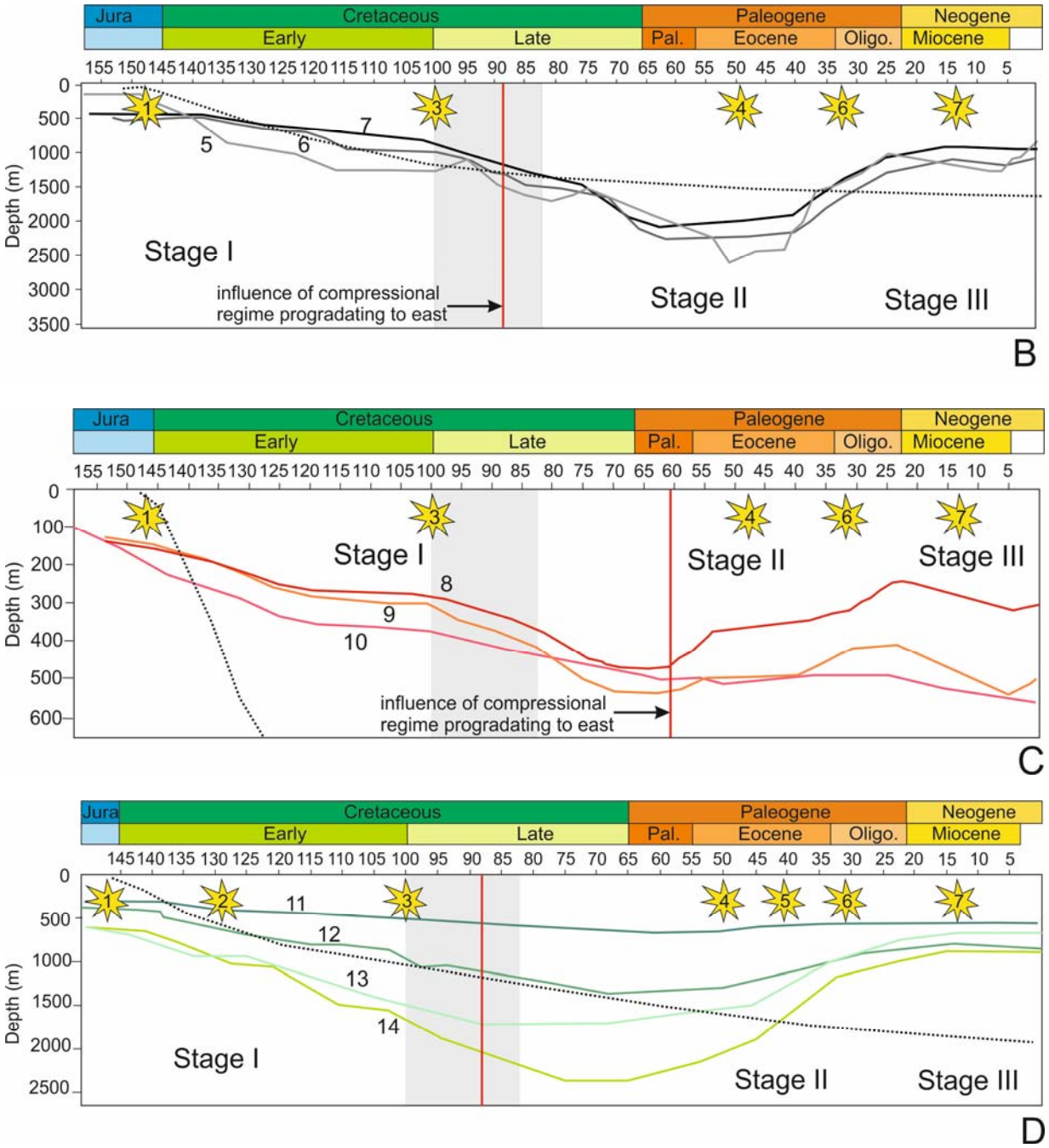

Figure 11 Tectonic subsidence curves for the (A) deep water phase during Jurassic to Mid/Late Cretaceous, (B) deep water during the Latest Cretaceous-Paleogene, (C) the marine platform during Jurassic to Late Cretaceous/Paleogene and (D) the deep water phase in the western Malvinas Basin, including main tectonic events. For locations see Figure 4. Black dashed curves show the theoretical subsidence, β-factor 1.3.

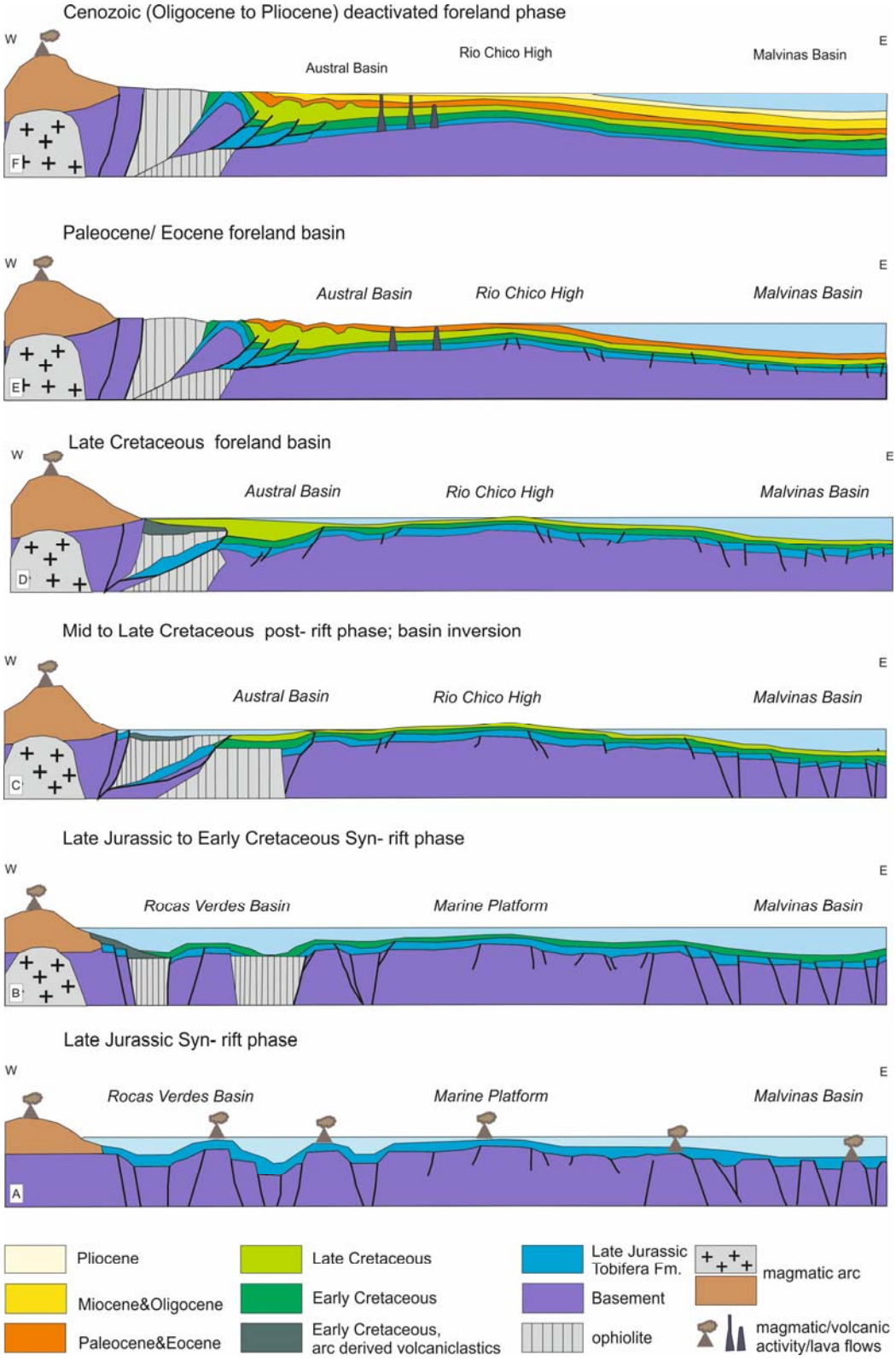

Figure 12 A-F: W-E sketches of the Austral Basin, the Rio Chico High and the western Malvinas Basin displaying the evolution stages of both basins since the Mid/Late Jurassic (not to scale). Details for the fold and thrust belt and the magmatic arc were modified from Wilson (1991).